Mathematical Medicine and Biology (2010) **27**, 39−74
doi:10.1093/imammb/dqp015
Advance Access publication on July 17, 2009

Continuum approximations of individual-based models for epithelial monolayers

J. A. FOZARD†, H. M. BYRNE, O. E. JENSEN AND J. R. KING
School of Mathematical Sciences, University of Nottingham, University Park, Nottingham NG7 2RD, UK

[Received on 16 October 2008; revised on 31 March 2009; accepted on 18 May 2009]

This work examines a 1D individual-based model (IBM) for a system of tightly adherent cells, such as an epithelial monolayer. Each cell occupies a bounded region, defined by the location of its endpoints, has both elastic and viscous mechanical properties and is subject to drag generated by adhesion to the substrate. Differential-algebraic equations governing the evolution of the system are obtained from energy considerations. This IBM is then approximated by continuum models (systems of partial differential equations) in the limit of a large number of cells, N, when the cell parameters vary slowly in space or are spatially periodic (and so may be heterogeneous, with substantial variation between adjacent cells). For spatially periodic cell properties with significant cell viscosity, the relationship between the mean cell pressure and length for the continuum model is found to be history dependent. Terms involving convective derivatives, not normally included in continuum tissue models, are identified. The specific problem of the expansion of an aggregate of cells through cell growth (but without division) is considered in detail, including the long-time and slow-growth-rate limits. When the parameters of neighbouring cells vary slowly in space, the $O(1/N^2)$ error in the continuum approximation enables this approach to be used even for modest values of N. In the spatially periodic case, the neglected terms are found to be $O(1/N)$. The model is also used to examine the acceleration of a wound edge observed in wound-healing assays.

Keywords: multicellular; homogenization; individual based; continuum; epithelial; monolayer.

1. Introduction

Epithelial tissues consist of sheets of tightly adherent cells with apicobasal polarization. These cover the internal and external surfaces of the body and one of their functions is to act as a barrier, regulating the migration of cells and chemicals across them (Alberts *et al.*, 2008). The study of such tissues is important not only because of their roles in wound healing (Martin, 1997) and morphogenesis (Schöck & Perrimon, 2002) but also because the majority of tumours in humans are epithelial in origin. During carcinogenesis in the colon, for example, cells mutate, colonize crypts and develop into a tumour in a complex series of events (Humphries & Wright, 2008); these involve interactions between multiple cells through mechanical forces, cell adhesion and cell signalling. As a consequence of this complexity, mathematical modelling is necessary to understand the entirety of the process (Anderson & Quaranta, 2008).

The cell is a natural unit of organization in a multicellular system. Models for such systems can be loosely divided into two categories: continuum models and individual- (or agent-) based models. Continuum models describe the properties of the cells in terms of locally averaged quantities (e.g. the number density of cells) whose evolution is governed by (partial) differential equations. Individual-based models (IBMs) take a contrasting approach, in which each cell is treated as a distinct entity, with

†Email: john.fozard@maths.nottingham.ac.uk

associated position and properties; these evolve according to rules which depend only on the internal state and local environment of each cell. There is much variation between IBMs, some of which are reviewed by Brodland (2004), and many different discrete models have been used to study epithelial tissues (e.g. Odell *et al.*, 1981; Weliky & Oster, 1990; Chen & Brodland, 2000; Meineke *et al.*, 2001; Nagai & Honda, 2001; Walker *et al.*, 2004; Galle *et al.*, 2005; Bindschadler & McGrath, 2007; van Leeuwen *et al.*, 2009).

The two types of models have relative advantages and disadvantages, the importance of which depends on the nature of the system and the biological question under consideration. Existing continuum models fail to resolve details on cellular or subcellular scales (Anderson, 2007), whereas it is relatively straightforward to include subcellular properties in the framework of an IBM (e.g. gene regulatory networks, van Leeuwen *et al.*, 2009, Ramis-Conde *et al.*, 2008; cytoskeletal dynamics, Marée *et al.*, 2006; cell cycle dynamics, Alarcón *et al.*, 2004; natural selection of cellular phenotypes, Hogeweg, 2000, Anderson, 2007) and cellular processes (e.g. juxtacrine signalling, Savill & Sherratt, 2003). Similarly, it is simpler to include heterogeneous cell populations in IBMs than in continuum models, and IBMs may be used to model small numbers of cells. However, techniques for the mathematical analysis of continuum models are better developed than those for IBMs. The computational expense of numerical simulations of IBMs depends upon the number of cells in the system, while for continuum models it depends upon the size of the system relative to the scale on which variations of interest occur, as this dictates the number of variables required for the spatial discretization to give a good approximation to the continuous solution.

Relating continuum models to IBMs in the limit of large numbers of cells is important for several reasons. As discussed above, continuum models may be substantially more efficient to simulate than IBMs, provided that the variations of interest occur over scales which are much larger than the size of the cells. Parameter estimation is a significant problem in biological modelling, and relating the two types of models may allow measurements of cell-scale properties to be used to estimate parameters in continuum models, and vice versa. The two types of models have largely been developed in isolation and connecting them may motivate developments in models of both kinds; the choices made in developing a continuum model (number of components, constitutive law, etc.) are often difficult to justify, while IBMs require many assumptions about the behaviour of individual cells. In particular, the study of IBMs will be useful in rationalizing phenomenological interaction terms such as those arising in multiphase models of tissue growth (Lemon *et al.*, 2006).

Continuum approximations of spatially discrete models have been of great interest in physical science, in particular, for lattice models such as the Fermi, Pasta and Ulam model (a chain of particles connected by non-linear springs). By expanding differences in Taylor series, a continuum approximation was obtained (Kruskal & Zabusky, 1964; Zabusky & Kruskal, 1965), exemplifying a procedure that is applicable in many such contexts (such as the approximation of discrete systems of master equations; Keck & Carrier, 1965); we will show how such approaches cen be extended to model heterogeneous cell populations below. We do so using homogenization methods (Bensoussan *et al.*, 1978; Pavliotis & Stuart, 2008), which have been applied to many physical processes, notably the solid mechanics of composite materials (Milton, 2002) and porous media (Hornung, 1997) when the properties of the medium vary on a small length scale. These methods have also been used in biological contexts, e.g. the bistable equation with heterogeneous conductivity as a model for wave propagation in cardiac tissue (Keener, 2000), models for neural networks (Bressloff, 2001), calcium dynamics in the cell cytoplasm (Goel *et al.*, 2006) and transport of diffusible substances in a line of coupled cells (Othmer, 1983). The aim of this procedure was to derive equations which govern the behaviour of the system over spatial scales which are much larger than those on which the material properties vary; the equations describing

large-scale behaviour are often the same as those for the small-scale problem, but with different effective constitutive relations (averaged over the short length scale). While such methods are more commonly applied to systems which are spatially continuous, we will here consider a system which is discrete in space; as noted in Kevrekidis *et al.* (2002), such discrete problems can typically be written as continuum problems with (heterogeneous) coefficients containing spatial delta functions.

Conversely, the approximation of spatially continuous models by discrete ones is fundamental to the numerical analysis of partial differential equations. While the spatial discretization is usually chosen because it gives a good approximation to the continuum problem, with the resulting discrete equations having favourable properties, related techniques used can be instructive in approximating discrete systems by continuous ones.

Continuum approximations of IBMs have been derived by a number of authors, the results obtained being specific to the particular models. In off-lattice centre-based models, each cell is described by the position of its centre, the cells exert forces on each other and the velocity of a cell centre is proportional to the applied force. A 1D model of this type, in which the force between cells depends on the distance between them (with optional additive noise) was examined by Bodnar & Velazquez (2005), and an integro-differential equation governing the cell densities was derived. Alt (2002) considered a 2D model in which only neighbouring cells interact (these being determined by the Voronoi diagram based on the cell centres), the forces between cells depending on the distance between them, the relative velocity and the length of the common side in the Voronoi tessellation; a continuity equation for the cell density and a Navier–Stokes-type force-balance equation with additive noise for the cell velocities were conjectured. This approximation has been derived rigorously for the 1D version of this model by Albeverio & Alt (2008). Drasdo (2005) derived a continuum approximation for an off-lattice centre-based IBM, which included cell division. Childress & Percus (1981) derived a continuum approximation of a 1D vertex-based IBM for a monolayer of homogeneous cells, in which the motion was driven by the adhesive surface energy of the cells; this is the work closest to what follows, but the latter includes cell elasticity, cell growth and heterogeneity in cellular properties.

The cellular Potts model (CPM) (Graner & Glazier, 1992), in which each cell is represented by a region containing multiple sites of a regular lattice, has also been used to investigate numerous biological systems (Merks & Glazier, 2005). Continuum approximations of this model for a single 1D cell have been obtained by Turner *et al.* (2004), and by Alber *et al.* (2007) for 2D cells (which are constrained to be rectangular) interacting through a chemoattractant and cell–cell adhesion, using a mean-field approximation. A non-linear diffusion equation describing the limit of high cell densities was discussed by Lushnikov *et al.* (2008).

The above models incorporate mechanical forces which act directly between cells. IBMs in which cells move randomly, interacting through a diffusible chemoattractant were considered by Stevens (2000) and Newman & Grima (2004); under certain conditions the classical Keller–Segal system can be obtained in the large cell-number limit. A discrete-lattice model for two randomly walking, competing cell populations was examined by de Masi *et al.* (2007) and approximated by a system of reaction-diffusion equations.

In this work, we will examine a particular 1D vertex-based IBM, as a precursor to studying higher dimensional systems (cf. the models of Weliky & Oster, 1990; Chen & Brodland, 2000; Nagai & Honda, 2001). The main aim of the paper will be to investigate the approximation of this deterministic IBM by continuum models. To illustrate the techniques used, the IBM considered will be intentionally simplistic, but motivated by the collective motion of adherent epithelia, such as in wound-healing experiments (Poujade *et al.*, 2007) or the growth of an epithelial colony (Haga *et al.*, 2005). Despite the limitations of the model, notably the lack of cell division (which we defer to later work) or membrane fluctuations,

we will use it to examine its predictions regarding the acceleration of the free edge of a monolayer, which is observed in wound-healing experiments (Poujade *et al.*, 2007).

The IBM will first be described in some detail in Section 2, where we discuss the underlying mechanical framework. As in the CPM, the motion is driven by a free energy or Hamiltonian, but unlike the CPM, explicit consideration is made of dissipative forces. The approximation of this IBM by a continuum model in the limit of a large number of cells is the subject of Section 3. We derive a continuum approximation when the cell parameters differ slowly between cells through replacing finite differences in the IBM by derivatives in a relatively straightforward fashion. We also consider cells with heterogeneous parameters, for which continuum approximations are obtained using a multiple scales approach. These are expressed in spatial variables in Section 4, permitting comparison with existing models; the continuum models derived from the IBM contain convective derivatives which are not usually included in models of this type. To assess the accuracy of these approximations, and to illustrate the behaviour of both the IBM and the continuum approximation, we use our model framework to study an aggregate that consists of expanding cells in Section 5, making a brief comparison between the behaviour of this IBM and some of the observations from wound-healing experiments in Section 5.5.

2. One-dimensional discrete model

We now give a detailed description of the one-dimensional IBM which is the subject of this paper.

2.1 *Geometrical representation*

We assume that each cell occupies a bounded interval; the cells adhere to each other and are unable to exchange positions with their neighbours. For N touching cells arranged along a line, we denote the positions of the $N+1$ vertices by $x_0, x_1, \ldots, x_N$, and the vertex velocities by $u_n = \mathrm{d}x_n/\mathrm{d}t$; the cells occupy the intervals $(x_0, x_1), (x_1, x_2), \ldots, (x_{N-1}, x_N)$, as illustrated in Fig. 1. Quantities associated with the cell lying between x_n and x_{n+1} are labelled with the subscript $n + \frac{1}{2}$ ($n = 0, \ldots, N-1$). The physical length of the cell is given by $l_{n+1/2} \equiv x_{n+1} - x_n$, so that

$$\frac{\mathrm{d}l_{n+1/2}}{\mathrm{d}t} = u_{n+1} - u_n, \qquad n = 0, \ldots, N-1. \tag{2.1}$$

The notation $\mathbf{x} = (x_0, \ldots, x_N)^T$ and $\mathbf{u} = (u_0, \ldots, u_N)^T$ will sometimes be used for brevity. The dependent variables of the system will comprise the vertex positions, $\mathbf{x}$ (or as the IBM will be invariant under translation, the cell lengths, $l_{n+1/2}$), and the 'target' (or 'natural') lengths of the cells, $a_{n+1/2}$, $n = 0, \ldots, N-1$; the latter will increase at a rate which possibly depends on the properties and environmental conditions of the cells.

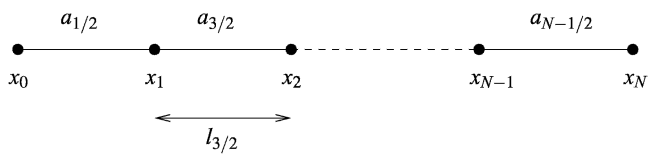

FIG. 1. Variables and geometry for the 1D vertex-based model.

2.2 *Energy gradient formulation*

As with many IBMs, such as the CPM (Graner & Glazier, 1992), vertex-based models (Nagai & Honda, 2001) or the 1D model of Childress & Percus (1981), we will consider the evolution of the system as being driven by the decrease in a notional mechanical free energy $H(\mathbf{x})$; we assume that H depends only on the vertex positions, as their speeds (and hence the corresponding kinetic energies) are small. This provides a convenient framework through which to derive force balances on individual vertices (boundaries between cells), although of course H does not explicitly incorporate the the constant turnover of chemical energy in cell maintenance and biochemical processes. However, chemical energy will be converted to mechanical energy by the cells in the course of growth; this will be included in the model later through parametric changes of some variables. Growth is often handled in a similar manner in the CPM (Glazier *et al.*, 2007). This energy is dissipated through various mechanisms, such as viscous forces in the cell cytoplasm and cytoskeleton, and the breaking of cell–cell (cadherin) and cell-substrate (integrin) adhesions. The net rate of energy dissipation is given by $\Phi(\mathbf{x}, \mathbf{u})$, which we require to be non-negative, vanishing only when $\mathbf{u} = \mathbf{0}$. The rate of change of energy is given as a function of $\mathbf{u}$ by

$$\frac{\mathrm{d}H}{\mathrm{d}t} = \mathbf{u} \cdot \nabla_{\mathbf{x}} H(\mathbf{x}),$$

where $\nabla_{\mathbf{x}} \equiv (\partial/\partial x_0, \partial/\partial x_1, \ldots, \partial/\partial x_N)^T$. Following Childress & Percus (1981), we assume that the system evolves such that $H(\mathbf{x})$ decreases most rapidly, under the constraint

$$\Phi(\mathbf{x}, \mathbf{u}) = -\mathbf{u} \cdot \nabla_{\mathbf{x}} H(\mathbf{x}), \tag{2.2}$$

on the velocity $\mathbf{u}$, which is that the rate of change of energy balances the dissipation rate. The velocity $\mathbf{u}$ which minimizes $\mathrm{d}H/\mathrm{d}t$, subject to (2.2), satisfies

$$\nabla_{\mathbf{x}} H(\mathbf{x}) + \eta \nabla_{\mathbf{u}} \Phi(\mathbf{x}, \mathbf{u}) = 0, \tag{2.3}$$

where η is a Lagrange multiplier enforcing (2.2) and $\nabla_{\mathbf{u}} \equiv (\partial/\partial u_0, \partial/\partial u_1, \ldots, \partial/\partial u_N)^T$. We take Φ to be a quadratic form in the vertex velocities,

$$\Phi(\mathbf{x}, \mathbf{u}) = \mathbf{u}^T \mathbb{D}(\mathbf{x}) \mathbf{u}, \tag{2.4}$$

(which is expected to be the case when the velocities are small, the resulting drag forces being linear functions of the vertex velocities) with $\mathbb{D}$ a symmetric matrix, in which case $\nabla_{\mathbf{u}} \Phi(\mathbf{x}, \mathbf{u}) = 2\mathbb{D}(\mathbf{x})\mathbf{u}$. Taking the dot product of (2.3) with $\mathbf{u}$, and subtracting (2.2), we find that $\eta = \frac{1}{2}$.

The potential and dissipation functions can be considered as exerting generalized forces on the vertices. The forces $\mathbf{F} = (F_0, F_1, \ldots, F_N)^T$ acting as a result of the potential are defined as

$$\mathbf{F} \equiv -\nabla_{\mathbf{x}} H(\mathbf{x}). \tag{2.5}$$

We term such forces 'static', as they are independent of the vertex velocities. The damping forces, $\mathbf{D} = (D_0, D_1, \ldots, D_N)^T$, generated by the dissipative processes are given (from 2.4) by

$$\mathbf{D} \equiv -\eta \nabla_{\mathbf{u}} \Phi(\mathbf{x}, \mathbf{u}) = -\mathbb{D}(\mathbf{x})\mathbf{u}.$$

With this notation (2.3) becomes

$$\mathbf{F} + \mathbf{D} = \mathbf{0}, \tag{2.6}$$

which can be thought of as force balances on the vertices. In the specific model developed below, the free energy and dissipation rate will both consist of a sum of contributions from individual cells, which depend only on the local properties and parameters of the cell. Each cell will exert static and drag forces on its end vertices, and so interacts directly only with its immediate neighbours.

2.2.1 *The energy function.* Many types of cells will adhere to and spread out upon a surface (assuming that the surface properties permit cell adhesion). This is a complicated process, involving a balance between extensional forces generated by the cell (through the extension of pseudopodia and adhesion to the substrate) and contractile forces actively generated by the cytoskeleton and as a result of its elasticity (Reinhart-King *et al.*, 2005). Here we make the simple assumption that it is energetically favourable for each cell, if isolated from its environment (but still adherent to a substrate), to attain its target length, $a_{n+1/2}$ (cf. the equilibrium area in the 2D vertex-based model of Nagai & Honda, 2001). This length performs the same role in the resulting model as the length of a cell in the zero-stress state for mathematical theories of tissue growth (e.g. Rodriguez *et al.*, 1994). A similar energy term is included in the CPM (Graner & Glazier, 1992) to enforce cell incompressibility. In some 2D models for epithelial cells (Chen & Brodland, 2000; Hilgenfeldt *et al.*, 2008), the cells are treated as having a fixed area in the plane of interest; in these models there is also a contribution to the energy from the cell perimeter as a result of the elastic properties of the cortical cytoskeleton.

The energy $H(\mathbf{x})$ will be taken to be a sum of contributions from each of the cells (depending only on local quantities), namely

$$H = \sum_{n=0}^{N-1} C(l_{n+1/2}, a_{n+1/2}; \lambda_{n+1/2}),$$

for some function $C(l, a; \lambda)$, where $\lambda_{n+1/2}$ parametrizes the mechanical properties of the n-th cell (here the cell elasticity and substrate adhesion). From (2.5), the static forces are then given by

$$F_n = p_{n-1/2} - p_{n+1/2}, \quad n = 0, \ldots, N, \tag{2.7}$$

where the cell 'pressures' $p_{n+1/2}$ are defined by

$$p_{n+1/2} \equiv -\frac{\partial C}{\partial l}(l_{n+1/2}, a_{n+1/2}; \lambda_{n+1/2}), \quad n = 0, \ldots, N-1.$$

While $p_{n+1/2}$ are introduced primarily for notational convenience, they correspond to the forces (per unit length in the transverse direction) that would be exerted by the cells upon their neighbours (normal to the interface between cells), were the vertices stationary. We have not yet defined $p_{-1/2}$ and $p_{N+1/2}$; these depend on the external forces acting on the end vertices.

One simple model for the energy of the cells, equivalent to a system of linear springs between the vertices, is given by

$$C(l, a; \lambda) = \frac{\lambda}{2}(a - l)^2, \quad p_{n+1/2} = \lambda_{n+1/2}(a_{n+1/2} - l_{n+1/2}), \quad n = 0, \ldots, N-1, \tag{2.8}$$

where $\lambda_{n+1/2} > 0$, so $p_{n+1/2} > 0$ whenever a cell is under compression ($a_{n+1/2} > l_{n+1/2}$). This linear model is likely to be reasonable for small deformations; however, it is not appropriate for situations where cells are highly compressed, when the pressure may exceed $\lambda_{n+1/2} a_{n+1/2}$.

2.2.2 *The energy dissipation rate.* In some works (Nagai & Honda, 2001), particularly where the equilibrium configurations are of primary concern, the dissipation rate is taken to be $\Phi = \mu \mathbf{u}^T \mathbf{u}/2$, with $\mu > 0$, the corresponding drag forces $\mathbf{D} = -\mu \mathbf{u}$ being proportional to the speed of the vertices. In this paper, we will consider a more general model. We assume that

$$\Phi = \sum_{n=0}^{N-1} G(u_n, u_{n+1}, l_{n+1/2}; \mu_{n+1/2}, \delta_{n+1/2}),$$

where $\mu_{n+1/2} > 0$ parametrizes the substrate drag of the n-th cell and $\delta_{n+1/2} \geqslant 0$ parametrizes its internal viscosity. The viscosity of a cell refers to the resistance of a cell to dynamic changes in shape through viscous dissipation in the cell cytoplasm and cytoskeleton. We model the energy dissipation of each cell as taking the form $G = G^s + G^v$, where G^s is the energy dissipated by drag between the cell and substrate and G^v is that dissipated by the internal viscosity of the cell. The corresponding drag force on the vertex x_n is $D_n = D_n^s + D_n^v$, where

$$D_n^{s,v} = -\frac{1}{2}\frac{\partial}{\partial u_n}\left(\sum_{m=\max(n-1,0)}^{\min(n,N)} G^{s,v}(u_m, u_{m+1}, l_{m+1/2}; \mu_{m+1/2}, \delta_{m+1/2}) \right).$$

The substrate exerts a drag on every point on the basal surface of the cell, the force per unit length being assumed proportional to the velocity, given by linearly interpolating the vertex velocities across the base of the cell. The associated energy dissipation is then

$$\begin{aligned} G^s(u_n, u_{n+1}, l_{n+1/2}; \mu_{n+1/2}) &= \mu_{n+1/2} \int_{x_n}^{x_{n+1}} u^2 \, \mathrm{d}x \\ &\simeq \mu_{n+1/2} \int_0^{l_{n+1/2}} \left(\frac{u_n(l_{n+1/2} - y) + u_{n+1} y}{l_{n+1/2}} \right)^2 \mathrm{d}y \\ &= \tfrac{1}{3} \mu_{n+1/2} l_{n+1/2} \left(u_n^2 + u_n u_{n+1} + u_{n+1}^2 \right). \end{aligned}$$

Summing the contributions from all cells, the drag forces are given by

$$D_n^s = -\frac{\mu_{n-1/2} l_{n-1/2}(u_{n-1} + 2u_n)}{6} - \frac{\mu_{n+1/2} l_{n+1/2}(2u_n + u_{n+1})}{6}, \quad n = 0, \ldots, N. \tag{2.9}$$

This formula holds for the end vertices ($n = 0$ and $n = N$) if we define $\mu_{-1/2} = 0$, $\mu_{N+1/2} = 0$.

In reality, the cells form a large number of dynamic adhesions with the substrate and actively exert forces upon it; in monolayers of proliferating cells these forces have been found to be mostly localized at the boundaries between cells (du Roure *et al.*, 2005). Experiments on wound healing in confluent monolayers of cells (Farooqui & Fenteany, 2005) have indicated that, while the cells generally remain adherent to each other at their apical (top) end, the individual cells extend lamellipodia at their base and actively crawl on the substrate, rather than being pulled or pushed along by their neighbours. However, we neglect such details here, and assume that the cells "slide" across the substrate.

The cells also dissipate energy as a result of their internal viscosity; this is modelled using

$$G^v(u_n, u_{n+1}, l_{n+1/2}; \delta_{n+1/2}) = \delta_{n+1/2}(u_{n+1} - u_n)^2 \tag{2.10}$$

for each cell, giving additional contributions of

$$D_n^v = \delta_{n+1/2}(u_{n+1} - u_n) - \delta_{n-1/2}(u_n - u_{n-1}), \quad n = 0, \ldots, N, \tag{2.11}$$

to the drag forces acting on each vertex (as would be generated by dashpots connecting the vertices of the cells). Expression (2.11) is valid for all n if we take $\delta_{-1/2} = \delta_{N+1/2} = 0$. An alternative approach of Childress & Percus (1981) is to consider the cells as being filled with a fluid of viscosity $\eta_{n+1/2}$, and to assume that each cell occupies a rectangle of fixed area $A_{n+1/2}$ in the cross section normal to the substrate. Further assuming that the extensional flow interpolates the velocities of the boundaries gives

$$G^{v*} = 4\eta_{n+1/2}A_{n+1/2}(u_{n+1} - u_n)^2/l_{n+1/2}^2. \tag{2.12}$$

We will not use this expression directly, but instead apply it later to estimate the typical size of the $\delta_{n+1/2}$; if we fix $l_{n+1/2}$ in (2.12) to be a typical cell length then it becomes of the same form as (2.10).

Using (2.7), (2.9) and (2.11), the force-balance equation (2.6) becomes, for $n = 0, \ldots, N$,

$$\frac{\mu_{n-1/2}l_{n-1/2}(u_{n-1} + 2u_n)}{6} + \frac{\mu_{n+1/2}l_{n+1/2}(2u_n + u_{n+1})}{6} - \delta_{n+1/2}(u_{n+1} - u_n) + \delta_{n-1/2}(u_n - u_{n-1}) = p_{n-1/2} - p_{n+1/2}. \tag{2.13}$$

2.3 *Cell elongation*

As indicated in Section 2.2, cellular metabolic processes do not fit naturally into the energy-gradient framework and will instead be modelled separately with additional equations and rules. To include cell elongation or flattening (growth without cell division), we will assume that the target lengths of the cells satisfy

$$\frac{\mathrm{d}a_{n+1/2}}{\mathrm{d}t} = \Gamma(l_{n+1/2}, p_{n+1/2}, a_{n+1/2}; \gamma_{n+1/2}), \quad n = 0, \ldots, N-1, \tag{2.14}$$

where $\gamma_{n+1/2}$ parametrizes the growth-related properties (elongation rate) of the n-th cell. As a simple model, we take

$$\Gamma(l, p, a; \gamma) = \gamma, \tag{2.15}$$

so the target length of the n-th cell increases at the constant rate $\gamma_{n+1/2}$; however, in comparisons with other models is it useful to consider other forms for the growth rate. We expect that cell elongation will, in general, be accompanied by cell division, but this process will be deferred to a later paper.

2.4 *Overview of model*

In summary, our IBM comprises (2.1), (2.8) and (2.14), which hold for each cell ($n = 0, \ldots, N-1$), and the force-balance equations (2.13), which hold for each vertex ($n = 0, \ldots, N$).

This differential-algebraic system contains a large number of subscripted quantities: the cell target lengths, $a_{n+1/2}$, and actual lengths, $l_{n+1/2}$, are differential variables (i.e. time derivatives appear explicitly), while the cell pressures, $p_{n+1/2}$, and vertex velocities, u_n, are algebraic variables (time derivatives do not appear explicitly). The remaining quantities $\mu_{n+1/2}$, $\delta_{n+1/2}$, $\lambda_{n+1/2}$ and $\gamma_{n+1/2}$ are non-negative parameters, which will all be assumed to be constant.

2.5 *Non-dimensionalization and parameter estimation*

We scale the cell parameters with typical values (denoted by asterisks)

$$\mu_{n+1/2} = \mu^* \hat{\mu}_{n+1/2}, \quad \lambda_{n+1/2} = \lambda^* \hat{\lambda}_{n+1/2}, \quad \delta_{n+1/2} = \delta^* \hat{\delta}_{n+1/2}, \quad \gamma_{n+1/2} = \gamma^* \hat{\gamma}_{n+1/2},$$

where we retain the possibility that properties may vary between cells. We scale the variables according to

$$a_{n+1/2} = a^* \hat{a}_{n+1/2}, \quad l_{n+1/2} = a^* \hat{l}_{n+1/2}, \quad p_{n+1/2} = \lambda^* a^* \hat{p}_{n+1/2}, \quad u_n = (\lambda^*/\mu^*)\hat{u}_n,$$

$$t = (\mu^* a^*/\lambda^*)\hat{t},$$

and the growth function by

$$\Gamma = \Gamma^* \hat{\Gamma},$$

where Γ^* is a typical value of Γ, and a^* is the typical length of a cell. With the growth law (2.15) one of Γ^* and γ^* is redundant, in which case we take them to be equal.

We will use only dimensionless quantities in the remainder of this paper and henceforth omit the hats from the dimensionless variables. The system of equations then becomes

$$\frac{\mu_{n-1/2} l_{n-1/2}(u_{n-1} + 2u_n)}{6} + \frac{\mu_{n+1/2} l_{n+1/2}(2u_n + u_{n+1})}{6}$$
$$- V\delta_{n+1/2}(u_{n+1} - u_n) + V\delta_{n-1/2}(u_n - u_{n-1}) = p_{n-1/2} - p_{n+1/2}, \tag{2.16a}$$

for $n = 0, \ldots, N$, and

$$p_{n+1/2} = \lambda_{n+1/2}(a_{n+1/2} - l_{n+1/2}), \tag{2.16b}$$

$$\frac{\mathrm{d}l_{n+1/2}}{\mathrm{d}t} = u_{n+1} - u_n, \tag{2.16c}$$

$$\frac{\mathrm{d}a_{n+1/2}}{\mathrm{d}t} = \alpha\Gamma(l_{n+1/2}, p_{n+1/2}, a_{n+1/2}; \gamma_{n+1/2}), \tag{2.16d}$$

for $n = 0, \ldots, N-1$, where

$$V = \delta^*/\mu^* a^*, \qquad \alpha = \Gamma^* \mu^*/\lambda^*, \tag{2.17}$$

are dimensionless parameters. Here V is the ratio of the drag due to the viscosity of the cells to that due to the substrate, and α is the ratio of the cell elongation rate (Γ^*/a^*) to the substrate–drag relaxation rate ($\lambda^*/\mu^* a^*$). The equations for the end vertices ($n = 0, N$) are that

$$\frac{\mu_{1/2} l_{1/2}(2u_0 + u_1)}{6} - V\delta_{1/2}(u_1 - u_0) = -p_{1/2}, \tag{2.18a}$$

$$\frac{\mu_{N-1/2} l_{N-1/2}(u_{N-1} + 2u_N)}{6} + V\delta_{N-1/2}(u_N - u_{N-1}) = p_{N-1/2}. \tag{2.18b}$$

Representative parameter values are listed in Table 1. Mi *et al.* (2007) proposed a 1D continuum model for the healing of a wound in a monolayer of intestinal epithelial cells (IEC-6); they considered

TABLE 1 *Parameter estimates for epithelial cells*

Parameter	Definition	Value	Source
a^*	Cell target length	10 μm	
h^*	Average cell height	6 μm	
μ^*	Cell–substrate drag constant	$0.01\,\mathrm{nN\,h/\mu m^3}$	Mi *et al.* (2007)
λ^*	Cell elastic constant	$0.4\,\mathrm{nN/\mu m^2}$	Mi *et al.* (2007)
δ^*	Cell viscosity constant	$7 \times 10^{-3}\,\mathrm{h\,nN/\mu m^2}$	(2.19)
Γ^*	Cell growth rate	0.07 μm/h	(2.20)
N	Number of cells	10–40	Poujade *et al.* (2007)

a layer of cells with linear elasticity and cell–substrate drag, which was pulled along by traction forces generated by cells at the free edge. Estimating the traction forces using measurements of Prass *et al.* (2006) of the force required to stall a migrating cell, and fitting the results of their model to the experimental data of Cetin *et al.* (2007), gave estimates of parameters which are equivalent to μ and λ in our model.

The model of Mi *et al.* (2007) did not include the effects of cell viscosity. We estimate δ^* using (2.12), and the approximate value $\eta \simeq 10^4\,\mathrm{Pa\,s}$ for the cell viscosity (Thoumine & Ott, 1997), from which we have

$$\delta^* = \frac{4\eta h^*}{a^*} \simeq 2 \times 10^4\,\mathrm{Pa\,s} \simeq 7\,\mathrm{Pa\,h} = 7 \times 10^{-3}\,\mathrm{h\,nN/\mu m^2}. \tag{2.19}$$

Before reaching confluence, IEC-6 cells have been observed to double in number every 20 h (Quaroni *et al.*, 1979). However, the growth rate may be significantly smaller within a monolayer because of contact inhibition; Corkins *et al.* (1999) suggested a doubling time of $T_d \simeq 72\,\mathrm{h}$. If we assume that the target length of a cell must increase from a size $a^*/2$ to a size a^* in this period, we obtain the estimate

$$\Gamma^* = \frac{a^*}{2T_d} \simeq 0.07\,\mathrm{\mu m/h}. \tag{2.20}$$

With these estimates, we find that the timescale for the dimensionless variables is $\mu^* a^*/\lambda^* \simeq 0.25\,\mathrm{h}$, and the dimensionless parameters describing the evolution of individual cells are approximately

$$\alpha \simeq 0.002, \qquad V \simeq 0.07, \tag{2.21}$$

although we expect there to be significant deviations from these values for different cell types and when individual cells are exposed to different environmental signals.

3. Continuum approximations

The approximation of the IBM (2.16) by continuum models in the large-cell-number limit is the focus of this paper. We first examine the case when the cell parameters vary slowly with respect to the cell index in Section 3.1, introducing appropriate scalings for the cell variables and parameters, and replacing the finite differences in the IBM by partial derivatives. To study this approximation in more detail, we compare the dispersion relationship for the continuum model with that for the IBM in Section 3.2.

To examine the case when cell parameters vary substantially between neighbouring cells, we consider cell properties which are periodic in the cell index in Section 3.3. When the cell viscosity is small,

the cell pressures and vertex velocities vary slowly with respect to the index and satisfy the same system of equations as for cells with properties that vary slowly in space. However, when the cells have significant viscosity, we find that the pressures of neighbouring cells differ substantially, with the relationship between the mean cell pressure and lengths depending upon the history of the cell lengths.

3.1 *Slowly varying approximation*

The IBM (2.16) has a similar form to a (semi-discrete or method of lines) finite-difference method for a particular system of partial differential equations. Such methods are usually considered in the limit of vanishing mesh size, in which case the solution of the discrete equations generally converges to the solution of the continuous equations. Here, the mesh size for the discrete equations is instead fixed. If variations in cellular variables occur over large numbers of cells, then the derivatives of the corresponding continuous functions are small, and so the (truncation) errors made in the approximation are also small; provided this slowly varying condition holds, the continuum system will be a good approximation to the discrete model.

The physical quantities associated with each cell (pressure, target length, etc.) are defined only at a finite set of points for the IBM. For a given quantity, $\phi_{n+1/2}$, we may extend the initial data (e.g. by band-limited interpolation; Trefethen, 2000) to a smooth function $\phi(\nu, t)$ (we use ν, rather than n, to denote the cell label in the continuous case) for $\nu \in [0, N]$, and we require that

$$\phi_{n+1/2} = \phi(n + \tfrac{1}{2}, 0), \quad n = 0, \ldots, N-1.$$

This will serve as initial data for the system of partial differential equations (3.2), to be described shortly; for $t > 0$ we expect that

$$\phi_{n+1/2} \simeq \phi(n + \tfrac{1}{2}, t), \quad n = 0, \ldots, N-1.$$

We may similarly extend the initial data for the vertex positions to a smooth function $x(\nu, t)$ on $[0, N]$, although we now require that $x_n = x(n, 0)$, $n = 0, \ldots, N$, and for $t > 0$ we have the approximation $x_n \simeq x(n, t)$, $n = 0, \ldots, N$. The continuous velocity $u(\nu, t)$ is then defined by $u(\nu, t) = \partial x/\partial t$, and we have $u_n \simeq u(n, t)$, $n = 0, \ldots, N$ for $t \geqslant 0$. We then expand all n-dependent quantities using their Taylor series, in (2.16a) about n, and in (2.16c) about $n + \frac{1}{2}$, as this minimizes the asymptotic order of the error in the approximation. Assuming that all quantities are slowly varying in ν, with variations typically occurring over $N \gg 1$ cells, we rescale

$$\nu = N\tilde{\nu}, \quad x = N\tilde{x}, \quad u = \tilde{u}/N, \quad t = N^2\tilde{t}, \quad V = N^2\tilde{V}, \quad \alpha = \tilde{\alpha}/N^2, \quad p = \tilde{p} \tag{3.1}$$

(these scalings of V and α constitute a distinguished limit). To leading order as $N \to \infty$ (in effect, retaining only the lowest derivatives that do not cancel in the Taylor expansions), (2.16) gives the following system of equations:

$$\mu l\tilde{u} - \tilde{V}\frac{\partial}{\partial\tilde{\nu}}\left(\delta\frac{\partial\tilde{u}}{\partial\tilde{\nu}}\right) = -\frac{\partial\tilde{p}}{\partial\tilde{\nu}}, \tag{3.2a}$$

$$\tilde{p} = \lambda(a - l), \tag{3.2b}$$

$$\frac{\partial l}{\partial\tilde{t}} = \frac{\partial\tilde{u}}{\partial\tilde{\nu}}, \tag{3.2c}$$

$$\frac{\partial a}{\partial\tilde{t}} = \tilde{\alpha}\,\Gamma(a, l, \tilde{p}, \gamma). \tag{3.2d}$$

The terms omitted from these expansions are of $O(N^{-2})$. We discuss the physical interpretation of (3.2) in Section 4.1, where we also consider these equations in Eulerian (spatial) rather than Lagrangian (cell-based) coordinates. The appropriate boundary conditions are given by the Taylor expansions of (2.18); with the current scalings these become

$$\tilde{p} = \tilde{V}\delta\frac{\partial\tilde{u}}{\partial\tilde{\nu}} \qquad \text{at } \tilde{\nu} = 0, 1, \tag{3.3}$$

where the omitted terms are again $O(N^{-2})$ provided that $\tilde{u}$ and $\tilde{p}$ satisfy (3.2a).

The dimensionless parameters $\tilde{\alpha}$ and $\tilde{V}$ for this rescaled system depend not only on the properties of the individual cells but also the on number of cells present, which will lie in the range $N = 10$ to $N = 1000$ for applications of interest here; in the wound-healing experiments of Poujade *et al.* (2007) the the system is 100–400 μm (roughly 10–40 cell diameters) across in the direction of interest. Assuming that the properties of individual cells are independent of monolayer size, we have $\tilde{\alpha} = 0.2$ and $\tilde{V} = 7 \times 10^{-4}$ for $N = 10$, while $\tilde{\alpha} = 2000$ and $\tilde{V} = 7 \times 10^{-8}$ for $N = 1000$. We note that with these estimates $\tilde{V}$ is small compared with $1/N$, which is the small parameter used in our continuum approximations. However, we retain the viscous terms in the continuum approximations in order for our model to be more generally applicable.

The IBM can be identified with a particular finite-element discretization of the continuum approximation (3.2), and (3.2) could also be derived directly from the energy-gradient formulation of the IBM; both these matters are discussed in more detail in Appendix A. From (A.1), the free energy $\tilde{H} = H/N$ and dissipation rate $\tilde{\Phi} = N\Phi$ associated with the continuum approximation are given by

$$\tilde{H} = \int_0^1 \frac{\tilde{p}^2}{2\lambda}\,\mathrm{d}\tilde{\nu}, \qquad \tilde{\Phi} = \int_0^1 \left\{\mu l\tilde{u}^2 + \tilde{V}\delta\left(\frac{\partial\tilde{u}}{\partial\tilde{\nu}}\right)^2\right\}\mathrm{d}\tilde{\nu}. \tag{3.4}$$

3.2 *Dispersion relationships for the IBM and the slowly varying continuum approximation*

To investigate how the scale on which cell properties (e.g. pressure and length) vary affects the validity of the continuum approximation, and to illustrate the properties of both models, we examine and compare the dispersion relationships for the IBM (2.16) and the continuum approximation (3.2). In the absence of cell elongation, $p_{n+1/2} = 0$ for all n is the only steady state of the IBM; as $H(\mathbf{x})$ is non-increasing in this case the trivial solution is stable.

We expect that short-wavelength modes will be poorly approximated as the derivatives of the solution, and hence the truncation errors, will not be small; as this is a local effect we will (just in this section) consider an infinite line of cells. With uniform cell parameters (i.e. $a_{n+1/2} = \mu_{n+1/2} = \lambda_{n+1/2} = \delta_{n+1/2} = 1$ for all n), the IBM (2.16) linearized about the steady state can be written as

$$\frac{1}{6}\left(\frac{\mathrm{d}p_{n-1/2}}{\mathrm{d}t} + 4\frac{\mathrm{d}p_{n+1/2}}{\mathrm{d}t} + \frac{\mathrm{d}p_{n+3/2}}{\mathrm{d}t}\right) - V\left(\frac{\mathrm{d}p_{n-1/2}}{\mathrm{d}t} - 2\frac{\mathrm{d}p_{n+1/2}}{\mathrm{d}t} + \frac{\mathrm{d}p_{n+3/2}}{\mathrm{d}t}\right)$$
$$= p_{n+3/2} - 2p_{n+1/2} + p_{n-1/2}$$

for all n. For modes of the form $p_{n+1/2} = \Re\left\{A_k(t)e^{ikn}\right\}$ (where admissible values of k lie in the range $0 \leqslant k \leqslant 2\pi$: if $k > 2\pi$ then the mode is identical to that with wavenumber $k \bmod 2\pi$, a phenomenon

known as aliasing, see e.g. Trefethen, 2000) we have that the decay rate of the amplitude, d_{IBM}, is given by

$$d_{\mathrm{IBM}} = -\frac{1}{A_k}\frac{\mathrm{d}A_k}{\mathrm{d}t} = \frac{12\sin^2\frac{k}{2}}{\left(1+2\cos^2\frac{k}{2}\right)+12V\sin^2\frac{k}{2}}.$$

(As $A_k(t)$ remains real if the initial value $A_k(0)$ is real, we may further restrict consideration to wavenumbers in the range $0 < k < \pi$ because $\cos((2\pi - k)n) = \cos(kn)$ for all integer n.)

Linearizing the continuum approximation (3.2) about the steady state $p = 0$ yields the pseudoparabolic equation

$$\left(1 - V\frac{\partial^2}{\partial\nu^2}\right)\frac{\partial p}{\partial t} = \frac{\partial^2 p}{\partial\nu^2}.$$

Equations of this type arise in the study of second-order fluids (Ting, 1963) and in the flow of liquid through fissured rock (Barenblatt *et al.*, 1960). For modes of the form $p = \Re\left\{A_k(t)e^{ik\nu}\right\}$, the decay rate of the amplitude is

$$d_C = -\frac{1}{A_k}\frac{\mathrm{d}A_k}{\mathrm{d}t} = \frac{k^2}{1+Vk^2}.$$

For the IBM, the decay rate d_{IBM} increases from 0 for $k = 0$ to a maximum value of $1/(V + 1/12)$ for $k = \pi$; for the continuum approximation, d_C increases from 0 for $k = 0$ to $1/V$ as $k \to \infty$. In the limit $k \to 0$, which corresponds to our slowly varying assumption, we have that

$$d_{\mathrm{IBM}} \sim k^2 + (\tfrac{1}{12} - V)k^4 + O(k^6), \quad d_C \sim k^2 - Vk^4 + O(k^6);$$

these decay rates agree to leading order, and so long-wavelength modes are well approximated. For $\tilde{V} \ll 1$, short-wavelength modes (varying over finite numbers of cells), which are poorly approximated by the continuum approximation, decay significantly more rapidly than those that vary on the scale of the whole aggregate (for which $k = O(N^{-1})$). When $\tilde{V} = V/N^2 = O(1)$, modes which vary over a finite number of cells and over the whole aggregate decay at comparable rates.

3.3 *Heterogeneous cell parameters*

The approximation of Section 3.1 is valid only if the cell variables and parameters vary slowly with respect to the cell index. However, we are also interested in cases for which there is substantial variation in parameters between adjacent cells. In this case, we adopt a multiple scales approach, allowing all variables to depend on both the discrete index, n, and the large length-scale variable, $\tilde{\nu}$. Through treating these as independent variables, expanding all dependent quantities in inverse powers of N and imposing solvability conditions at each order, a system of partial differential equations for the dependent variables is obtained. The analysis is presented in more detail in Appendix B, and we summarize the results below. In order for the method used to be well grounded, we restrict attention to situations in which the cell properties are periodic in the cell index $n + 1/2$, with period $M = O(1)$—this allows us to pursue a multiple scales analysis that is traditional in periodic homogenization. However, we discuss the application of these continuum models to problems with less well-structured cell properties. We also only consider the case where the growth rate is constant for each cell ($\Gamma \equiv \gamma$).

When $\tilde{V} = 0$, we find in Appendix B.1 that the cell pressures, $p_{n+1/2}$, and vertex velocities, $u_{n+1/2}$, at leading order depend on the index only through the large-scale variable $\tilde{\nu}$. Provided that $\mu_{n+1/2}$ is

not correlated with any of the other parameters (i.e. that the average of the product of the two quantities is equal to the product of the averages), we recover (3.2) for the leading-order cell pressures, vertex velocities and mean cell lengths, but with all parameters replaced by their average values over a period (which we denote by an overline), except for $\lambda_{n+1/2}$ for which the appropriate average is the harmonic mean $1/\overline{(1/\lambda_{n+1/2})}$. The drag forces and growth rates for a group of cells combine linearly, which explains the use of the arithmetic mean for $\mu_{n+1/2}$ and $\gamma_{n+1/2}$. That the appropriate average for the stiffness $\lambda_{n+1/2}$ is the harmonic mean can be understood by considering a group of compressed cells at uniform pressure: the length of each cell will be less than its target length by an amount proportional to $1/\lambda_{n+1/2}$, and so the least stiff cells are the most compressed. The boundary conditions (3.3) again hold in this case (to leading order), as do the expressions (3.4), but with all parameters replaced by their appropriate averages and the cell lengths replaced by their mean values.

The viscous case ($\tilde{V} = O(1)$) is examined in Appendix B.2. While the leading-order vertex velocities again vary slowly with respect to the discrete index, the cell pressures are found to differ substantially between neighbouring cells. The mean cell lengths $\bar{l}(\tilde{\nu}, \tilde{t})$, the mean target lengths $\bar{a}(\tilde{\nu}, \tilde{t})$ and the vertex velocities, $\tilde{u}(\tilde{\nu}, t)$, satisfy (to leading order)

$$\bar{\mu}\bar{l}\tilde{u} - \frac{\partial}{\partial\tilde{\nu}}\left(\kappa\frac{\partial\tilde{u}}{\partial\tilde{\nu}}\right) = -\frac{\partial}{\partial\tilde{\nu}}\left(\kappa\overline{\left(\frac{\tilde{p}}{\tilde{V}\delta}\right)}\right), \tag{3.5a}$$

$$\frac{\partial\bar{l}}{\partial\tilde{t}} = \frac{\partial\tilde{u}}{\partial\tilde{\nu}}, \tag{3.5b}$$

$$\frac{\partial\bar{a}}{\partial\tilde{t}} = \tilde{\alpha}\bar{\gamma}, \tag{3.5c}$$

provided that $\mu_{n+1/2}$ is not correlated with any of the other cell parameters, where $1/\kappa = \overline{(1/\tilde{V}\delta)}$. However, the relationship between the mean cell pressures and cell lengths cannot be directly obtained from the average of (2.16b), as $\tilde{p}_{n+1/2}$ and $l_{n+1/2}$ are correlated with $\lambda_{n+1/2}$, $\delta_{n+1/2}$ and $\gamma_{n+1/2}$. Instead, we must consider M additional equations

$$\tilde{q}_{m+1/2} - \tilde{V}\delta_{m+1/2}\left(\tilde{\alpha}\gamma_{m+1/2} - \frac{1}{\lambda_{m+1/2}}\frac{\partial\tilde{q}_{m+1/2}}{\partial\tilde{t}}\right) = \kappa\left\{\overline{\left(\frac{\tilde{p}}{\tilde{V}\delta}\right)} - \frac{\partial\tilde{u}}{\partial\tilde{\nu}}\right\}, \tag{3.5d}$$

which govern the pressures $\tilde{q}_{m+1/2}(\tilde{\nu}, \tilde{t})$, $m = 0, \ldots, M-1$ of each of the cells in the periodic unit. The left-hand side of (3.5d) is (an approximation to) $p_{n+1/2} - \tilde{V}\delta\mathrm{d}l_{n+1/2}/\mathrm{d}\tilde{t}$, which is the total force exerted by a cell on its neighbours; as the right-hand side of (3.5d) is independent of m, we see that it is this quantity which differs only slightly between adjacent cells, while the pressure may vary substantially. Note that the $\tilde{q}_{m+1/2}$ are functions of the continuous cell index $\tilde{\nu}$ and so (3.5d) consists of M partial differential equations (of the same form as (3.5b)) that are coupled to (3.5a)–(3.5c).

In (3.5a) and (3.5d), the average of the pressures is given by

$$\overline{\left(\frac{\tilde{p}}{\tilde{V}\delta}\right)} = \frac{1}{M}\sum_{m=0}^{M-1}\frac{\tilde{q}_{m+1/2}(\tilde{\nu}, \tilde{t})}{\tilde{V}\delta_{m+1/2}}. \tag{3.5e}$$

The pressures $\tilde{p}_{n+1/2}$ of the cells in the IBM are related to the $\tilde{q}_{m+1/2}$ through

$$\tilde{p}_{n+1/2}(\tilde{t}) \simeq \tilde{q}_{n(\mathrm{mod}\ M)+1/2}\left(\frac{n+\frac{1}{2}}{N}, \tilde{t}\right).$$

The boundary conditions for (3.5) are that

$$\overline{\left(\frac{\tilde{p}}{\tilde{V}\delta}\right)} = \frac{\partial \tilde{u}}{\partial \tilde{\nu}} \qquad \text{at } \tilde{\nu} = 0, 1. \tag{3.6}$$

Equations (3.5d) provide a relationship between cell pressures and lengths, and are equivalent to simulating an aggregate of M cells at each point $\nu \in [0, 1]$, where the cells have no cell–substrate drag, and the end vertices move such that the aggregate is expanding at a rate $M\partial\tilde{u}/\partial\tilde{\nu}$.

To illustrate the need for (3.5d)–(3.5e), we consider the behaviour of this problem with constant expansion rate $\partial\tilde{u}/\partial\tilde{\nu}$, in which case the cell pressures can be found to be linear functions of time in the long-time limit. However, the cell pressures relax to this solution on an $O(\tilde{V})$ timescale, and so when $\tilde{t} = O(1)$ and $\tilde{V} = O(1)$ we cannot treat the problem as being in quasi-equilibrium.

The above results were derived under the assumption that the cell properties were periodic with respect to the cell index, with this period being much smaller than the total number of cells. While it is relatively straightforward to extend this analysis to cell properties which are locally periodic, but vary on a long length scale, this seems to be an unrealistic model for a heterogeneous collection of cells. Nevertheless, we believe that the resulting continuum approximation is applicable to less regularly structured cell properties; this belief is borne out by numerical experiments (reported below). When $\tilde{V} = 0$, we expect that the same equations will hold as in the periodic case, but with the average over a period (overbars) interpreted as a 'local' average over cells that are large in number but comprise a small fraction of the cell population (e.g. $O(N^{1/2})$). When $\tilde{V} = O(1)$, we expect that (3.5a)–(3.5c) will still hold with the average over a period replaced by the local average. However, rather than solving (3.5d) for the pressures of each of the cells in a period, we instead examine $\tilde{q}(\tilde{\nu}, \tilde{t}; \delta, \gamma, \lambda)$, which is the local distribution of the pressure as a function of the cell parameters. This satisfies

$$\tilde{q} - \tilde{V}\delta\left(\tilde{\alpha}\gamma - \frac{1}{\lambda}\frac{\partial \tilde{q}}{\partial \tilde{t}}\right) = \kappa\left\{\overline{\left(\frac{\tilde{p}}{\tilde{V}\delta}\right)} - \frac{\partial \tilde{u}}{\partial \tilde{\nu}}\right\}, \tag{3.7}$$

the average (3.5e) being replaced by

$$\overline{\left(\frac{\tilde{p}}{\tilde{V}\delta}\right)} = \iiint W(\delta, \lambda, \gamma)\frac{\tilde{q}(\tilde{\nu}, \tilde{t}; \delta, \lambda, \gamma)}{\tilde{V}\delta}\,\mathrm{d}\delta\,\mathrm{d}\gamma\,\mathrm{d}\lambda, \tag{3.8}$$

where $W(\delta, \lambda, \gamma)$ is the local distribution of cell properties, the integral in (3.8) being over the support of W. The equations (3.7)–(3.8) can be seen to reduce to (3.5d)–(3.5e) in the spatially periodic case.

4. Spatial form of the continuum approximations, and comparison with existing models

The continuum approximations are now written in terms of spatial variables. We start by discussing the features of these equations and then compare them with existing continuum models of growing multicellular tissues, paying particular attention to the slow-elongation limit.

4.1 *Spatial form of the continuum approximations*

The use of the (Lagrangian) cell index ν as an independent variable in the continuum model hinders comparison with existing models. Instead, we transform the independent variables from (ν, t) to (x, t),

where $x(\nu, t)$ is the physical (Eulerian) position of the vertex with index ν (corresponding to x_n in the discrete model). On the population scale, we write $x = N\tilde{x}$, and $\tilde{x}(\tilde{\nu}, \tilde{t})$ satisfies

$$\left(\frac{\partial \tilde{x}}{\partial \tilde{\nu}}\right)_{\tilde{t}} = l, \qquad \left(\frac{\partial \tilde{x}}{\partial \tilde{t}}\right)_{\tilde{\nu}} = \tilde{u}$$

(cf. $\mathrm{d}x_n/\mathrm{d}t = u_n$ for the discrete equations). In spatial variables, (3.2) becomes

$$\mu\tilde{u} - \tilde{V}\frac{\partial}{\partial \tilde{x}}\left(\delta l \frac{\partial \tilde{u}}{\partial \tilde{x}}\right) = -\frac{\partial \tilde{p}}{\partial \tilde{x}}, \tag{4.1a}$$

$$\tilde{p} = \lambda(a - l), \tag{4.1b}$$

$$\frac{\mathrm{D}l}{\mathrm{D}\tilde{t}} = l\frac{\partial \tilde{u}}{\partial \tilde{x}}, \tag{4.1c}$$

$$\frac{\mathrm{D}a}{\mathrm{D}\tilde{t}} = \tilde{\alpha}\Gamma(a, l, \tilde{p}; \gamma), \tag{4.1d}$$

where we have introduced the convective derivative

$$\frac{\mathrm{D}}{\mathrm{D}\tilde{t}} \equiv \frac{\partial}{\partial \tilde{t}} + \tilde{u}\frac{\partial}{\partial \tilde{x}}.$$

Thus,

$$\frac{\mathrm{D}\phi}{\mathrm{D}\tilde{t}} = 0, \tag{4.1e}$$

for any property ϕ which is constant in time for a particular cell (e.g. λ, δ, γ and μ). These equations hold on $\tilde{x}_L < \tilde{x} < \tilde{x}_R$, where (3.3) becomes

$$\tilde{p} = \tilde{V}\delta l\frac{\partial \tilde{u}}{\partial \tilde{x}} \quad \text{at } \tilde{x} = \tilde{x}_L, \tilde{x}_R, \tag{4.2}$$

and the boundaries move with the local cell velocity $\tilde{u}$, so $\mathrm{d}\tilde{x}_{L,R}/\mathrm{d}\tilde{t} = \tilde{u}(\tilde{x}_{L,R}, \tilde{t})$.

We note that the transport of other cellular properties (such as protein concentrations) may be modelled using equations similar to (4.1e); if $c_{n+1/2}$ is a cellular property satisfying $\mathrm{d}c_{n+1/2}/\mathrm{d}\tilde{t} = F(c_{n+1/2})$ (e.g. c could be the level of a protein with intracellular production rate $F(c)$), and which varies slowly with the cell index, then the appropriate equation in spatial coordinates is

$$\frac{\mathrm{D}c}{\mathrm{D}\tilde{t}} = F(c).$$

The restriction that the cell properties vary slowly with the cell index is essential; a different approach would be needed when this is not the case (e.g. for cell cycle models).

Using (4.1b)–(4.1d), rewrite (4.1c) as

$$\tilde{\alpha}\Gamma - l\frac{\partial \tilde{u}}{\partial \tilde{x}} = \frac{1}{\lambda}\frac{\mathrm{D}\tilde{p}}{\mathrm{D}\tilde{t}}, \tag{4.3}$$

from which we see that the convective derivative of the cell pressure is also contained in this model. While this convective derivative appears in the continuum model derived from an IBM by Childress & Percus

(1981) or implicitly in models formulated in Lagrangian coordinates (e.g. Mi *et al.*, 2007), many other extant models neglect such contributions. Defining the cell density by $\rho = 1/l$, (4.1c) is equivalent to

$$\frac{\partial \rho}{\partial \tilde{t}} + \frac{\partial}{\partial \tilde{x}}(\rho \tilde{u}) = 0,$$

corresponding to conservation of cell number.

When $\tilde{V} = 0$, (4.1a) reduces to Darcy's law (used to model the flow of a viscous fluid through a porous medium); similar pressure–velocity relationships have been used in incompressible fluid models for solid tumours (Greenspan, 1976), although the biological system considered here is a 2D sheet of cells lying on a substrate rather than a 3D spheroid. When $\tilde{V} > 0$, there is an additional term of Brinkman viscosity form corresponding to the extensional viscosity of the cells in (4.1a), and a similar term in the boundary condition (4.2).

We may apply the same transformation from cell-based variables to spatial variables for heterogeneous cell parameters, but for brevity we omit the resulting equations here.

4.2 *Comparison with other models in the slow-elongation limit*

We now approximate (4.1) in the slow-elongation limit $\tilde{\alpha} \ll 1$ (with $\tilde{V} = O(1)$ or smaller), which (from the estimates of Section 3.1) we expect to be appropriate for relatively small numbers of cells; this limit may also be appropriate for larger numbers of cells of a different type, or if there is significant inhibition of growth within the layer. The appropriate timescale is $\tilde{t} = O(1/\tilde{\alpha})$ as the cells grow by a finite amount over this long period. The cell pressures and vertex velocities should be of equal order to balance terms in (4.1a), and from (4.3) we see that $\tilde{p} = O(\tilde{\alpha})$ and $\tilde{u} = O(\tilde{\alpha})$. We rescale using

$$\tilde{p} = \tilde{\alpha}\check{p}, \quad \tilde{u} = \tilde{\alpha}\check{u}, \quad \tilde{t} = \check{t}/\tilde{\alpha}, \tag{4.4}$$

in which case we have to leading order $l = a + O(\alpha)$ and

$$\mu\check{u} - \tilde{V}\frac{\partial}{\partial \tilde{x}}\left(\delta a \frac{\partial \check{u}}{\partial \tilde{x}}\right) = -\frac{\partial \check{p}}{\partial \tilde{x}}, \tag{4.5a}$$

$$a\frac{\partial \check{u}}{\partial \tilde{x}} = \Gamma, \tag{4.5b}$$

$$\frac{\mathrm{D}a}{\mathrm{D}\check{t}} = \Gamma, \quad \frac{\mathrm{D}\phi}{\mathrm{D}\check{t}} = 0, \quad \phi = \lambda, \mu, \delta, \gamma, \tag{4.5c}$$

$$\text{where} \quad \frac{\mathrm{D}}{\mathrm{D}\check{t}} \equiv \frac{\partial}{\partial \check{t}} + \check{u}\frac{\partial}{\partial \tilde{x}}, \tag{4.5d}$$

with boundary conditions (4.2) at $\tilde{x} = \tilde{x}_L$ and $\tilde{x} = \tilde{x}_R$, the boundaries moving with the local cell velocity $\check{u}$; the convective derivative of the cell pressures on the right-hand side of (4.3) is small in this limit. Differentiating (4.5a) with respect to $\tilde{x}$ gives

$$\frac{\Gamma}{a} - \tilde{V}\frac{\partial}{\partial \tilde{x}}\left(\frac{1}{\mu}\frac{\partial}{\partial \tilde{x}}(\delta\Gamma)\right) = -\frac{\partial}{\partial \tilde{x}}\left(\frac{1}{\mu}\frac{\partial \check{p}}{\partial \tilde{x}}\right),$$

with the boundary conditions $\check{p} = \tilde{V}\delta\Gamma$, $\tilde{x} = \tilde{x}_L, \tilde{x}_R$, which is an elliptic problem for the cell pressures at each moment in time. This approximation will be valid for $\check{t} = O(1)$; for small time there will be transient behaviour in which the solution evolves from the initial data to a quasi-equilibrium state.

If $\Gamma \equiv \gamma\, lS(\check{p}) \simeq \gamma\, aS(\check{p})$ (so that the source term per unit length is a function of pressure alone), the system (4.5) becomes

$$\gamma\left\{S(\check{p}) - \tilde{V}\frac{\partial}{\partial\tilde{x}}\left(\frac{1}{\mu}\frac{\partial}{\partial\tilde{x}}\left(\delta a S(\check{p})\right)\right)\right\} = -\frac{\partial}{\partial\tilde{x}}\left(\frac{1}{\mu}\frac{\partial\check{p}}{\partial\tilde{x}}\right), \quad \frac{\partial\check{u}}{\partial\tilde{x}} = \gamma\, S(\check{p}),$$
$$\frac{\mathrm{D}a}{\mathrm{D}\check{t}} = \gamma\, aS(\check{p}), \quad \frac{\mathrm{D}\phi}{\mathrm{D}\check{t}} = 0,$$

along with the boundary conditions $\check{p} = \tilde{V}\delta\gamma\, aS(\check{p})$ at $\tilde{x} = \tilde{x}_L, \tilde{x}_R$. When $\tilde{V} = 0$, this is similar in form to the single-phase incompressible fluid models developed by Greenspan (1976) to describe the growth of a (3D) cellular aggregate. Many other models exist for solid tumours, some of which are reviewed by Araujo & McElwain (2002) and Roose *et al.* (2007). Sheets of cells have been less well studied using continuum models; along with those mentioned previously (Childress & Percus, 1981; Mi *et al.*, 2007), there are also reaction-diffusion models (Sherratt & Murray, 1990), those which consider cells moving within an elastic tissue (Murray & Oster, 1984; Tranquillo & Murray, 1992; Olsen *et al.*, 1995) (comprising a force balance equation for the whole tissue and conservation equations for cell densities), and models which treat an epithelium as a growing elastic beam (Edwards & Chapman, 2007).

5. Expansion of a cellular island

We now consider the expansion of an island of cells caused by an increase in their target lengths (cell expansion). We examine the validity of the continuum approximations as the number of cells in the IBM varies and discuss the effects of cell heterogeneity. We also consider the behaviour of the models in the small-growth-rate and long-time limits. Rather than give an exhaustive description of the behaviour of the system in all possible parameter regimes, we instead illustrate its behaviour for a few choices of parameter values.

5.1 *Parameters, initial data and continuum approximations*

In the simulations, the growth rate (rate of increase of the target length, a) will be taken to be constant in time for each cell ($\Gamma \equiv \gamma$). For uniform cell parameters, through an appropriate choice of scales in our non-dimensionalization, we set $\lambda_{n+1/2} = \delta_{n+1/2} = \mu_{n+1/2} = \gamma_{n+1/2} = 1$ and take the initial target lengths to be $a_{n+1/2} = 1$ at $t = 0$ for all cells, so that $a_{n+1/2}(\tilde{t}) = 1 + \tilde{\alpha}\tilde{t}$ from (3.2d). The initial positions of the vertices are taken to be

$$x_n = n - \tfrac{N}{2}, \qquad n = 0, \ldots, N,$$

so all cells are uncompressed ($p_{n+1/2} = 0$) and have unit length ($l_{n+1/2} = 1$), the aggregate occupying the region $-N/2 < x < N/2$. In the heterogeneous case, the cell parameters and initial target lengths are taken to be $\delta_{n+1/2} = \mu_{n+1/2} = 1$ and $a_{n+1/2}(0) = 1$ for all cells, but $\lambda_{n+1/2}$ and $\gamma_{n+1/2}$ are periodic in the cell index (with period 4) as listed in Table 2. The cell target lengths are then $a_{n+1/2} = 1 + \tilde{\alpha}\gamma_{n+1/2}\tilde{t}$, with the mean being $\bar{a} = 1 + \tilde{\alpha}\tilde{t}$. The initial vertex positions, x_n, are again chosen such that all cells have zero pressure, the aggregate occupying the region $-N/2 < x < N/2$. Solutions to these discrete problems depend upon time t, the dimensionless parameters α and V, and the number of cells N.

For both slowly varying and heterogeneous cell parameters (in the latter case, for $\tilde{V} \ll 1$), the cell lengths can be eliminated from the continuum approximation, giving

$$(1 + \tilde{\alpha}\tilde{t} - \tilde{p})\tilde{u} - \tilde{V}\frac{\partial^2\tilde{u}}{\partial\tilde{\nu}^2} = -\frac{\partial\tilde{p}}{\partial\tilde{\nu}}, \quad \tilde{\alpha} - \frac{\partial\tilde{p}}{\partial\tilde{t}} = \frac{\partial\tilde{u}}{\partial\tilde{\nu}}, \tag{5.1}$$

TABLE 2 *Cell parameter values used for the heterogeneous problems:* $\delta_{n+1/2} = \mu_{n+1/2} = 1$ *for all cells, while the cell elastic constants,* $\lambda_{n+1/2}$*, and growth rates,* $\gamma_{n+1/2}$*, are as shown for* $s = 0, \ldots, (N-4)/4$*, with period* $M = 4$

n	$4s$	$4s+1$	$4s+2$	$4s+3$
$\gamma_{n+1/2}$	3/2	1/2	3/2	1/2
$\lambda_{n+1/2}$	2/3	2/3	2	2

on $0 < \tilde{\nu} < 1$, with boundary conditions

$$\tilde{p} = \tilde{V}\frac{\partial \tilde{u}}{\partial \tilde{\nu}} \quad \text{at } \tilde{\nu} = 0, 1, \tag{5.2}$$

and initial data $\tilde{p} = 0$ at $\tilde{t} = 0$. For heterogeneous cell parameters with significant cell viscosity ($\tilde{V} = O(1)$), the cell viscosities are taken to be uniform ($\delta_{n+1/2} = 1$ for all n) for simplicity; the continuum approximation (3.5) can be written as

$$\left(1 + \tilde{\alpha}\tilde{t} - \overline{\left(\frac{\tilde{q}_{m+1/2}}{\lambda_{m+1/2}}\right)}\right)\tilde{u} - \tilde{V}\frac{\partial^2 \tilde{u}}{\partial \tilde{\nu}^2} = -\frac{\partial \overline{\tilde{q}}}{\partial \tilde{\nu}}, \tag{5.3a}$$

$$\frac{1}{\tilde{V}}(\tilde{q}_{m+1/2} - \overline{\tilde{q}}) - \tilde{\alpha}\gamma_{m+1/2} + \frac{1}{\lambda_{m+1/2}}\frac{\partial \tilde{q}_{m+1/2}}{\partial \tilde{t}} = -\frac{\partial \tilde{u}}{\partial \tilde{\nu}}, \quad m = 0, \ldots, M-1, \tag{5.3b}$$

on $0 < \tilde{\nu} < 1$, with boundary conditions

$$\overline{\tilde{q}} = \tilde{V}\frac{\partial \tilde{u}}{\partial \tilde{\nu}} \qquad \text{at } \tilde{\nu} = 0, 1,$$

and the initial data $\tilde{q}_{m+1/2} = 0$, $m = 0, \ldots, M-1$. While we solve the problem (numerically) in cell-based variables, the transformation to spatial coordinates, $\tilde{x}(\tilde{\nu}, \tilde{t})$, is given by the solution of $\partial \tilde{x}/\partial \tilde{t} = \tilde{u}$ with initial data $\tilde{x} = \tilde{\nu} - 1/2$ at $\tilde{t} = 0$. The solution $\tilde{p}(\tilde{\nu}, \tilde{t})$, $\tilde{u}(\tilde{\nu}, \tilde{t})$ and $\tilde{x}(\tilde{\nu}, \tilde{t})$ (or $\tilde{q}_{m+1/2}(\tilde{\nu}, \tilde{t})$, $m = 0, \ldots, M-1$, $\tilde{u}(\tilde{\nu}, \tilde{t})$ and $\tilde{x}(\tilde{\nu}, \tilde{t})$) depends only on $\tilde{\alpha}$ and $\tilde{V}$. In general, we are unable to find an explicit solution to the initial-boundary value problems (5.1) and (5.3), but instead approximate them numerically using a semi-discrete Galerkin finite-element method, as described in Appendix A.

5.2 *Uniform cell parameters*

We examine numerical simulations of the IBM (2.16)–(2.18) and the continuum model (5.1)–(5.2) in Figures 2 and 3, without and with cell viscosity, respectively. In both cases, we find that the total size of the aggregate and the maximum cell pressure increase with time. In Figure 2, there is no cell viscosity ($\tilde{V} = 0$); the vertex velocities are approximately linear in $\tilde{\nu}$ (or $\tilde{x}$), and the pressure profile is approximately parabolic, driving the motion of the cells. The pressure is greatest in the centre of the aggregate, as the aggregate expands symmetrically about its centre. Figure 3 shows that, with viscosity ($\tilde{V} = 1$), the pressure profile is still approximately parabolic, but now contains a uniform component that increases with time and is needed to overcome the internal viscosity of the cells as they expand. The velocity profile is still approximately linear in the cell index $\tilde{\nu}$, but the maximum cell speed now increases (noticeably) with time. Both with and without cell viscosity, we find that the differences between the IBM and the continuum approximation at $\tilde{t} = 1$ (and with $\tilde{\alpha} = 1$) scale like N^{-2}. Even for

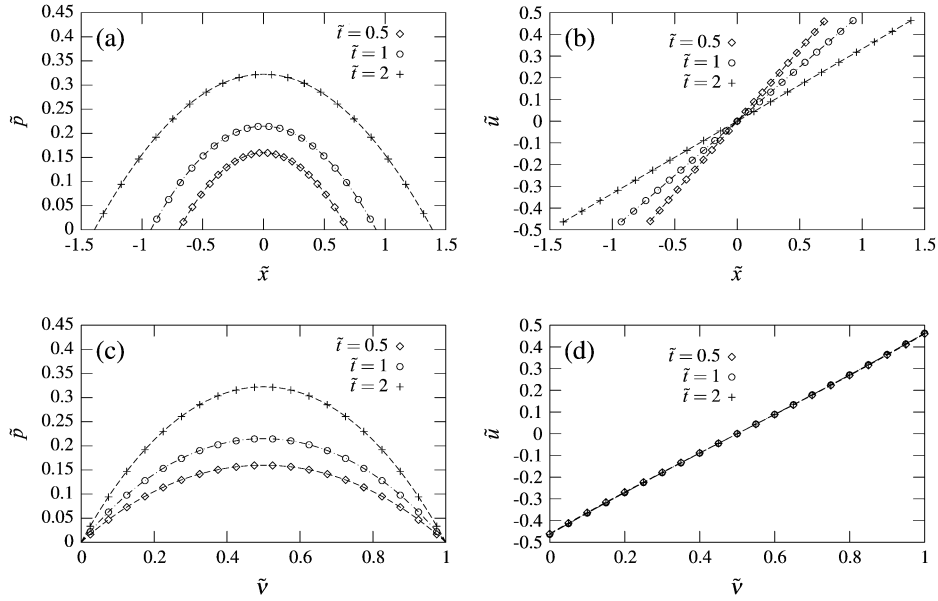

FIG. 2. Expansion of a homogeneous aggregate of $N = 20$ cells without cell viscosity ($\tilde{V} = 0$), extending at a constant rate ($\Gamma \equiv 1$), and with expansion rate parameter $\tilde{\alpha} \equiv N^2\alpha = 1$. Results are displayed in rescaled variables $\tilde{x} \equiv x/N$, $\tilde{v} \equiv v/N$, $\tilde{u} \equiv u/N$, $\tilde{p} \equiv p$, and the solutions are evaluated at $\tilde{t} \equiv t/N^2 = 0.5, 1, 2$. The markers show the pressures at the midpoints of the cells, $\tilde{p}_{n+1/2}$, in (a) and (c) and the velocities of the vertices, $\tilde{u}_n$, in (b) and (d) computed using the IBM (2.16)–(2.18), while the broken lines are numerical simulations of the continuum approximation (5.1)–(5.2). Plots (a) and (b) show the solution in terms of the spatial variable $\tilde{x}$, while (c) and (d) show the solution in terms of the cell-index variable $\tilde{v}$.

$N = 5$ cells, the IBM and the continuum approximation are in close agreement, with the maximum absolute errors in $\tilde{p}$ and $\tilde{u}$ (with $\tilde{\alpha} = 1$ and at $\tilde{t} = 1$) being approximately 4×10^{-3} and 1×10^{-4} without viscosity ($\tilde{V} = 0$), or 5×10^{-4} and 3×10^{-5} with cell viscosity ($\tilde{V} = 1$).

As discussed in Section 4.2, the continuum approximation simplifies to (4.5) in the limit $\tilde{\alpha} \ll 1$; in this case it is appropriate to examine the solution in the rescaled variables $\check{p}$, $\check{u}$ and $\check{t}$, as defined by (4.4). The reduced system (4.5) has the exact solution

$$\check{p} = \frac{1+\check{t}}{2}\left\{\frac{1}{4} - \frac{\tilde{x}^2}{(1+\check{t})^2}\right\} + \tilde{V}, \quad \check{u} = \frac{\tilde{x}}{1+\check{t}}, \quad -\frac{1+\check{t}}{2} \leqslant \tilde{x} \leqslant \frac{1+\check{t}}{2}. \tag{5.4}$$

We compare numerical simulations of the IBM, the continuum approximation (5.1)–(5.2), and (5.4) at $\tilde{t} = 1$ in Figure 4, where we confirm that the models approach the solution (5.4) in the limit $\tilde{\alpha} \to 0$, both with and without cell viscosity.

5.3 *Heterogeneous cell parameters*

In this section, we consider cells with heterogeneous parameters, as listed in Table 2. Without cell viscosity ($\tilde{V} = 0$), the IBM and continuum approximation (5.1)–(5.2) can be seen in Fig. 5 to be in reasonable agreement, even when the number of cells is moderate ($N = 8$). The solution to the continuum approximation is symmetric about $\tilde{x} = 0$, but the solution to the IBM is shifted to the left; this higher order correction is a consequence of the asymmetry of the cell parameters in each period.

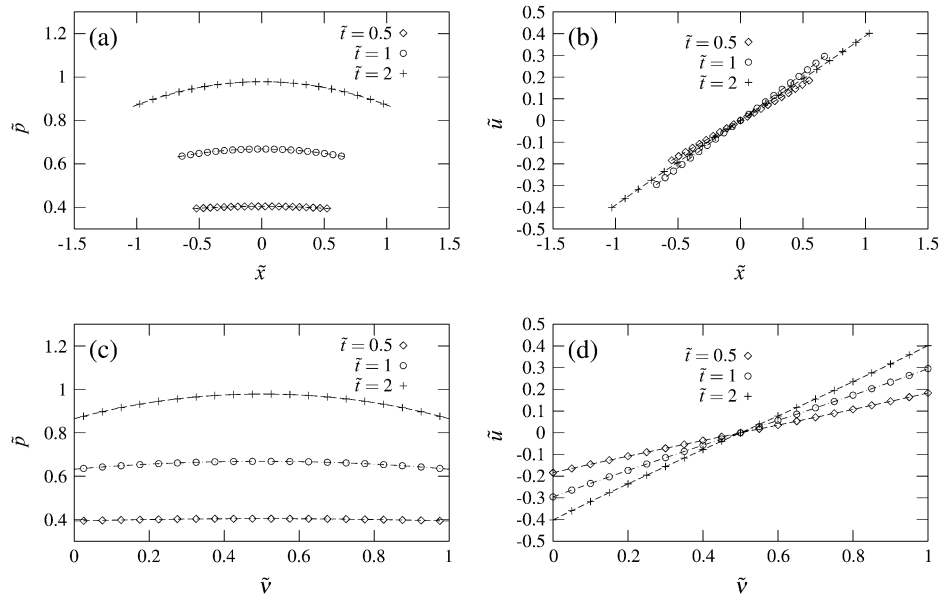

FIG. 3. Expansion of a homogeneous aggregate of cells; as in Fig. 2 but with cell viscosity ($\tilde{V} = 1$).

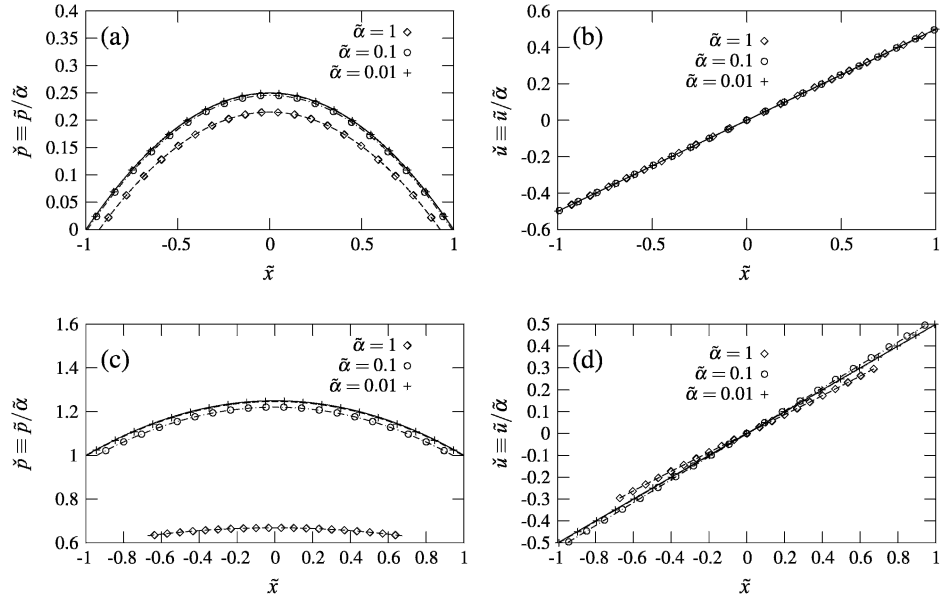

FIG. 4. Small growth rate behaviour of the IBM and continuum approximation for an aggregate of $N = 20$ cells, with varying values of $\tilde{\alpha}$; the solutions are displayed in the rescaled variables $\tilde{x} \equiv x/N$ and $\check{p} \equiv \tilde{p}/\tilde{\alpha} \equiv p/N^2\alpha$ in (a) and (c), or $\check{u} \equiv \tilde{u}/\tilde{\alpha} \equiv u/N\alpha$ in (b) and (d), all solutions being evaluated at $\check{t} \equiv \tilde{\alpha}\tilde{t} \equiv \alpha t = 1$. Plots (a) and (b) show the behaviour without cell viscosity ($\tilde{V} = 0$), while (c) and (d) are with cell viscosity ($\tilde{V} = 1$). The broken lines show the solution of the continuum approximation (5.1)–(5.2) for each value of $\tilde{\alpha}$, while the solid line is the approximation (5.4), valid in the limit $\tilde{\alpha} \to 0$.

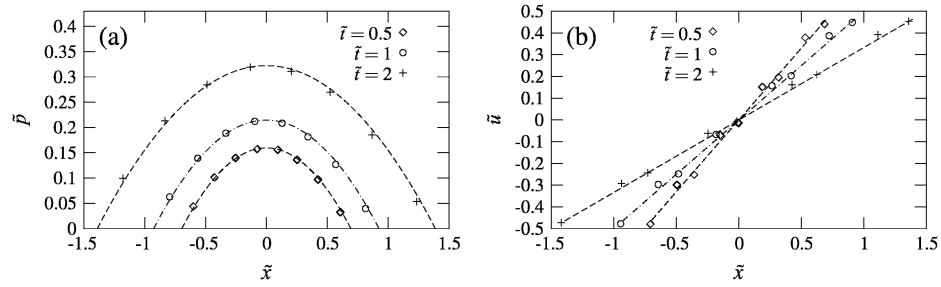

FIG. 5. Expansion of an inviscid aggregate of ($N = 8$) cells; as in Fig. 2 (a) and (b), but with periodic cell properties as listed in Table 2.

When $\tilde{V} = O(1)$, the leading-order cell pressures depend on the discrete index n, while the leading-order vertex velocities depend on the discrete index only through the large length-scale variable $\tilde{v}$. This can be seen in Fig. 6, where we examine the solution of the IBM at a single point in time: the cell pressures are oscillatory in space, while the vertex velocities differ only slightly between neighbouring vertices. This is compared with the simulations of (5.3), which yields approximations $\tilde{q}_{m+1/2}$, $m = 0, \ldots, M-1$, to the pressures of the $M = 4$ cells in each period. Both with and without cell viscosity, the maximum absolute difference between the IBM and the continuum approximation is found to be $O(N^{-1})$ for large N. This error has a spatially oscillating component caused by local variation in cellular parameters and a smooth component needed for the solution to satisfy the discrete boundary conditions (2.18).

To confirm our belief that the continuum approximation does not require periodicity of cell parameters, we examine the simple case in which the parameters of the cells are as in Table 2, but with the four cells in each period permuted randomly. The cell parameter distribution $W(\delta, \lambda, \mu)$ is the same as in the periodic case, namely,

$$W(\delta, \lambda, \mu) = \frac{1}{M} \sum_{m=0}^{M-1} d(\delta - \delta_{m+1/2}) d(\lambda - \lambda_{m+1/2}) d(\mu - \mu_{m+1/2}),$$

where $d(\cdot)$ denotes the delta function; (3.7) and (3.8) reduce to (3.5d) and (3.5e), respectively. The

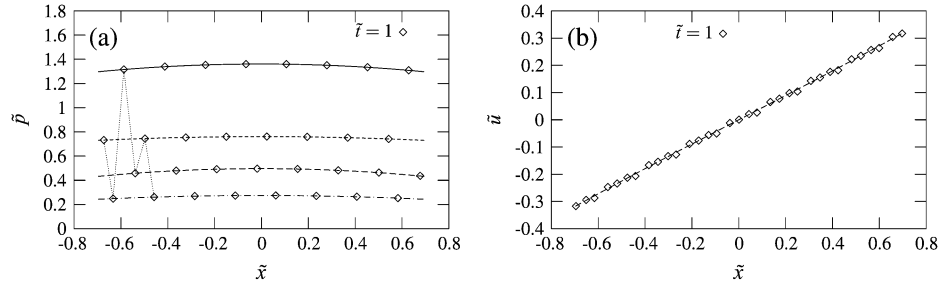

FIG. 6. Expansion of an aggregate of cells with periodic cell properties; as in Fig. 5, but for $N = 32$ cells with viscosity ($\tilde{V} = 1$). The markers show the pressures at the midpoints of the cells (a) and the vertex velocities (b) in the IBM (2.16)–(2.18), evaluated at $\tilde{t} = 1$. In (a), we plot the solutions $\tilde{q}_{1/2}$ (short dashes), $\tilde{q}_{1+1/2}$ (dash-dotted), $\tilde{q}_{2+1/2}$ (solid) and $\tilde{q}_{3+1/2}$ (long dashes) of the continuum approximation (5.3), which are the pressures of the cells in each period ($\tilde{p}_{n+1/2} \simeq \tilde{q}_{n(\mathrm{mod}\ M)+1/2}((n+\frac{1}{2})/N, \tilde{t})$); we also plot a dotted line joining the pressures at the centres of the first six cells to emphasise the spatial oscillations.

results of these simulations are shown in Fig. 7, where the continuum approximation and IBM can again be seen to be in reasonable agreement; for the simulations with $\tilde{V} = 0$ the error is noticeably larger than in Fig. 5, although we note that the number of cells ($N = 8$ cells, corresponding to two groups of four cells) is not overly large.

The behaviour in the slow growth rate ($\tilde{\alpha} \ll 1$) limit is also of interest. In the absence of cell viscosity ($\tilde{V} = 0$), the leading-order behaviour is given by (5.4), just as for uniform cell parameters. When the cells have significant viscosity ($\tilde{V} = O(1)$), on rescaling $\tilde{q}_{m+1/2} = \tilde{\alpha}\check{q}_{m+1/2}$ and all other variables following (4.4), (5.3) become

$$\check{u} - \tilde{V}\frac{\partial^2 \check{u}}{\partial \tilde{y}^2} = -\frac{\partial \overline{\check{q}}}{\partial \tilde{y}}, \tag{5.5a}$$

$$\check{q}_{m+1/2} - \overline{\check{q}} = \tilde{V}\left(\gamma_{m+1/2} - \frac{\partial \check{u}}{\partial \tilde{y}}\right), \quad m = 0, \ldots, M-1 \tag{5.5b}$$

to leading order. Taking the average of (5.5b) over a period gives

$$\frac{\partial \check{u}}{\partial \tilde{y}} = 1 \tag{5.6}$$

(as $\overline{\gamma} = 1$ here), so the pressures of the individual cells are related to the mean pressure $\overline{\check{q}}$ through

$$\check{q}_{m+1/2} = \overline{\check{q}} + \tilde{V}(\gamma_{m+1/2} - 1), \quad m = 0, \ldots, M-1, \tag{5.7}$$

the local variations in cell pressure being caused by differences in growth rates, and so viscous forces. The solution to (5.5a) and (5.6) is given by (5.4) with $\check{p}$ replaced by the average cell pressure $\overline{\check{q}}$. We note

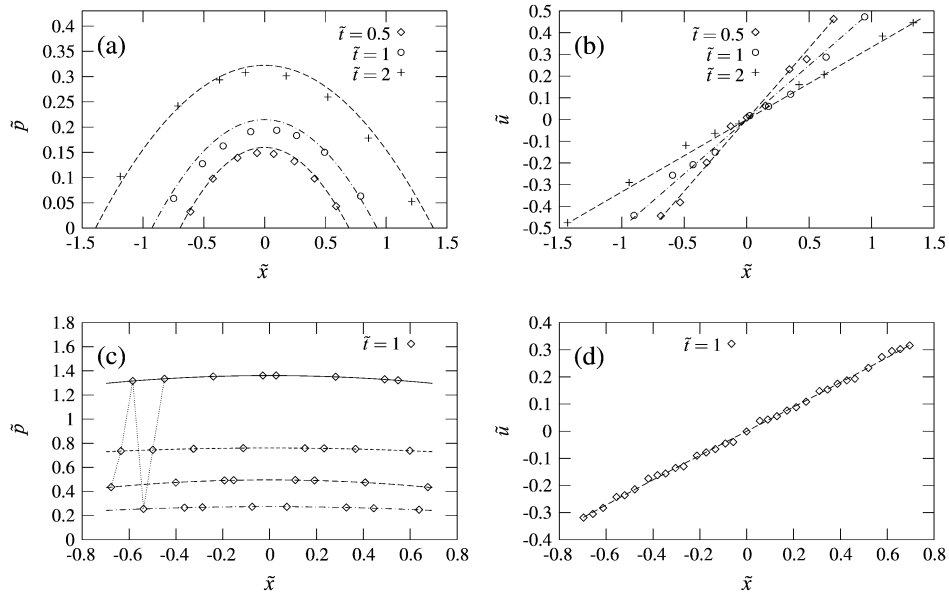

FIG. 7. Expansion of aggregates of cells with non-periodic heterogeneous cell properties; for (a) and (b) without viscosity ($\tilde{V} = 0$) and $N = 8$ cells as in Fig. 5, and for (c) and (d), with cell viscosity ($\tilde{V} = 1$) and $N = 32$ cells as in Fig. 6, but with the parameters in each period of four cells permuted randomly.

that the continuum approximation greatly simplifies in this limit, as (5.3b) has the explicit (approximate) solution (5.7).

5.4 *Long-time behaviour*

Finally, we briefly examine the long-time behaviour of solutions to (5.1). Posing the ansatz $\tilde{p} = \tilde{\alpha}\tilde{t}P(\tilde{\nu})$, $\tilde{u} = U(\tilde{\nu})$ and $\tilde{x} = \tilde{\alpha}\tilde{t}X(\tilde{\nu})$, we have from (5.1) that

$$(1-P)U = -\frac{\mathrm{d}P}{\mathrm{d}\tilde{\nu}}, \quad \tilde{\alpha}(1-P) = \frac{\mathrm{d}U}{\mathrm{d}\tilde{\nu}}, \quad \frac{\mathrm{d}X}{\mathrm{d}\tilde{\nu}} = 1-P, \quad X(\tfrac{1}{2}) = 0,$$

to leading order in $\check{t}$, with the boundary conditions $P = 0$ at $\tilde{\nu} = 0, 1$, and the symmetry condition $X(1/2) = 0$. This has solution

$$P = 1 - B - \frac{\tilde{\alpha}X^2}{2}, \quad U = \tilde{\alpha}X, \qquad X = \sqrt{\frac{2B}{\tilde{\alpha}}}\tan\left(\sqrt{\frac{B\tilde{\alpha}}{2}}\left(\tilde{\nu} - \tfrac{1}{2}\right)\right), \tag{5.8}$$

for some constant B determined by the boundary conditions $P = 0$ at $\tilde{\nu} = 0$ and $\tilde{\nu} = 1$: for $\tilde{\alpha} \ll 1$, we have $B \sim 1 - \tilde{\alpha}/8$; for $\tilde{\alpha} \gg 1$, it is found that $B \sim 2\pi^2(1 - 4\sqrt{2/\tilde{\alpha}})/\tilde{\alpha}$. The cell viscosity, $\tilde{V}$, does not affect the leading-order solution in this limit (provided that $\check{t} \gg \tilde{V}$). We plot simulations of the IBM and the continuum approximation (5.1)–(5.2) in these similarity variables in Fig. 8, where they can be seen to approach (5.8) in the long-time limit. The simulations in Fig. 8 are the same cases as those in Figs 2 and 3, but evaluated at later time points.

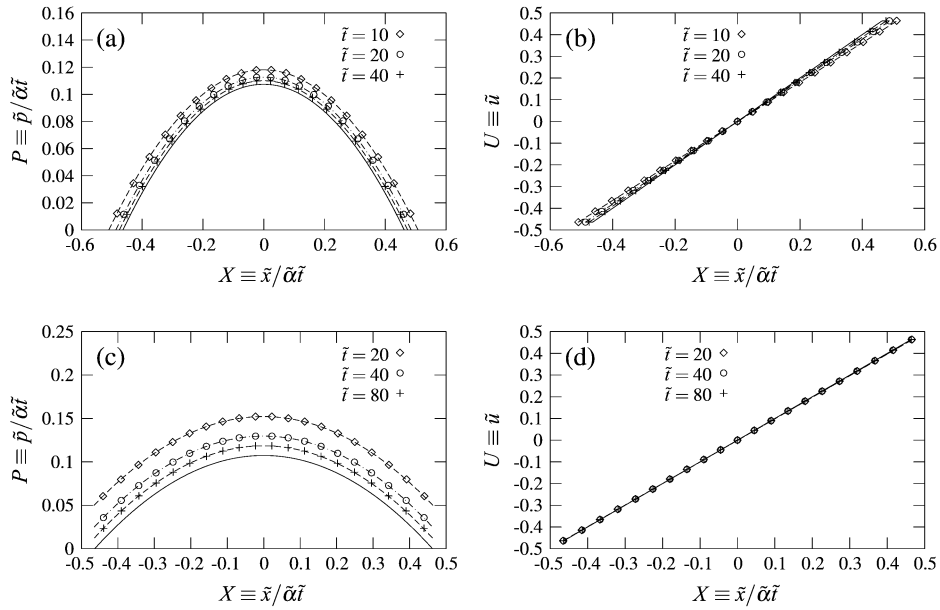

FIG. 8. Long-time behaviour for the expansion of an island of cells (with $N = 20$ cells and $\tilde{\alpha} = 1$), plotted in the similarity variables $P \equiv \tilde{p}/\tilde{\alpha}\tilde{t}$, $U \equiv \tilde{u}$ and $X \equiv \tilde{x}/\tilde{\alpha}\tilde{t}$, with $\tilde{V} = 0$ in (a) and (b) and $\tilde{V} = 1$ in (c) and (d); the solid line is the asymptotic solution (5.8), where for $\tilde{\alpha} = 1$ we have that $B \simeq 0.893$.

For heterogeneous cell parameters, we find that the long-time behaviour is the same as with uniform cell parameters (the cell pressures being slowly varying to leading order even for $\tilde{V} = O(1)$). However, the IBM can be observed numerically to break down in this limit; the maximum pressure grows like $\tilde{\alpha}\tilde{t}P(1/2)$, while the maximum pressure which can be sustained by a cell (with the model (2.8) for the cell mechanical properties) is $\lambda_{n+1/2}(1 + \tilde{\alpha}\gamma_{n+1/2}\tilde{t})$. As $P(1/2)$ is an increasing function of α, with $P(1/2) = 0$ for $\alpha = 0$ and $P(1/2) \to 1$ as $\tilde{\alpha} \to \infty$, the lengths of some cells become negative if $\tilde{\alpha}$ is sufficiently large (namely if $P(1/2) > \min(\gamma_{m+1/2}\lambda_{m+1/2})$; in the simulations of Fig. 8 the cell parameters are uniform so this is not the case).

5.5 *Wound-healing assays*

The migration of cells can be investigated using 'wound-healing' assays, in which a confluent epithelium is made to have a free edge, either by scratching the layer with a razor blade or pipette cone or by removing a stencil which previously confined the cells (Poujade *et al.*, 2007). Some epithelial cell lines (e.g Madin-Darby canine kidney cells) maintain cell-cell contacts and migrate collectively as a sheet, in which case the mean distance travelled by the free edge is a superlinear (approximately quadratic) function of time (Rosen & Misfeldt, 1980; Farooqui & Fenteany, 2005) (although the speed of the edge may level off after several days, as suggested by Rosen & Misfeldt, 1980). While cell division does occur in such an assay (Poujade *et al.*, 2007), with the total number of cells increasing linearly with time, similar results for the first 10 h after wounding have been obtained with mitotically inhibited cells.

In Fig. 9, we examine the velocity of the right-hand edge of an island of $N = 20$ identical cells, with expansion rate parameter $\tilde{\alpha} = 1$ and a variety of values for the cell viscosity parameter, $\tilde{V}$. (The lines for $\tilde{V} = 0$ and $\tilde{V} = 1$ correspond to the simulations of Figs 2 and 3, respectively.) In all cases, the speed of the edge increases with time. In the absence of cell viscosity ($\tilde{V} = 0$), this acceleration is associated with the establishment of a parabolic pressure profile in the layer; for the continuum approximation, the speed of the edge is found to be proportional to $\tilde{t}^{1/2}$ for small time. Cell viscosity acts to further slow the development of a pressure gradient in the aggregate, reducing the initial acceleration; the behaviour for small dimensionless time may partly explain the roughly uniform acceleration observed in experiments. The velocity of the edge tends towards a constant value for sufficiently large time (see (5.8)) as

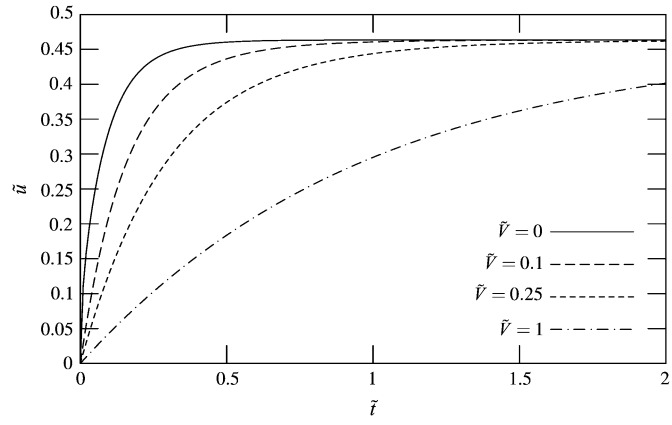

FIG. 9. The velocity of the right-hand edge of an expanding island of cells (with $N = 20$ and $\tilde{\alpha} = 1$), for a variety of different values of the cell viscosity parameter, $\tilde{V}$. The results are displayed in the rescaled dimensionless variables $\tilde{u} \equiv u/N$ and $\tilde{t} \equiv t/N^2$.

a consequence of the fixed number of cells and the constant growth rates. The present model therefore provides a mechanistic description of the superlinear growth seen experimentally.

6. Discussion

In this paper, we have presented a simple 1D IBM for a layer of adherent cells. Continuum models which approximate its behaviour in the limit of large numbers of cells were derived, both when the cell parameters vary slowly in space and when they are heterogeneous (and periodic); most previous works which derive a continuum model from an IBM assume that all cells are identical. In the former case, we were able to replace finite differences in the IBM by partial derivatives in the resulting continuum model. In the latter case, we adopted a multiple scales approach; when the cell viscosity was small ($\tilde{V} \ll 1$), we found that the cell pressures and vertex velocities varied slowly in space. The continuum approximation with heterogeneous parameters took the same form as in the slowly varying case, but with all cell parameters replaced by their appropriate averages; for the cell stiffness $\lambda_{n+1/2}$, this was not the arithmetic mean $\overline{\lambda_{n+1/2}}$, but rather the geometric mean $1/\overline{(1/\lambda_{n+1/2})}$. However, when the cells have significant viscosity ($\tilde{V} = O(1)$) and heterogeneous parameters, the pressures of neighbouring cells may differ substantially, and the relationship between mean cell lengths and pressures is found to depend upon the history of the solution; the local problem relaxes to a steadily expanding state on a timescale which is comparable to that on which the large-scale problem evolves. As a consequence, a group of cells (without cell–substrate adhesion) must be simulated at each point in space to obtain the effective constitutive relation.

The resulting continuum models (apart from that for the heterogeneous problem with cell viscosity) resemble existing incompressible fluid models for cell growth, but with the addition of Brinkman viscosity terms and convective derivatives of the cell pressures. From the parameter estimation in Section 2.5, it seems likely that the viscous terms are small, but the convective derivatives (often ignored in continuum models of growing tissues; e.g. Greenspan, 1976; Byrne & Chaplain, 1996) may be significant. The continuum models provide good approximations to the IBM, even for moderate ($N = 5$) numbers of cells. Furthermore, the continuum approximation facilitates the analysis of the system in the slow-growth-rate and long-time limits.

The IBM considered here was intentionally simplistic to illustrate the techniques involved in the derivation of continuum approximations. As each cell is treated as a distinct entity in the IBM, it is straightforward to include subcellular processes, e.g. regulatory networks modelled by systems of ordinary differential equations, such as those controlling planar cell polarization (Klein & Mlodzik, 2005). We reiterate that the continuum approximation of Section 4.1 is justifiable only when the state of the cellular processes varies slowly between neighbouring cells; when this is not the case, e.g. in patterning through juxtacrine signalling (Owen *et al.*, 2000) or for models of the cell cycle (Novák & Tyson, 2004), a more sophisticated approach is necessary. The mechanical model used for the cells could also be increased in complexity—in particular, the treatment of cell–cell and cell–substrate adhesion could be made more physically realistic. Active cell migration could also be included in this model by the addition of terms (namely the chemotactic potential) to the free energy of the cells (as discussed by Glazier *et al.*, 2007 for the CPM). However, the most significant process which is lacking in the current IBM is cell division. Cell division complicates the model, as the number of discrete entities in the system (and so the number of variables in the IBM) increases, requiring relabelling of the cells in both the IBM and the continuum approximation (in cell-based coordinates). Furthermore, cells are unlikely to divide in synchrony, causing local variation in cell sizes and providing additional motivation for our study of the IBM with heterogeneous cell parameters.

This IBM is a 1D analogue of the 2D or 3D vertex-based models of Nagai & Honda (2001) and Chen & Brodland (2000); it is clearly desirable to extend the analysis of this paper to higher dimensions. However, this is significantly complicated by the fact that the neighbours of a given cell are not fixed but may change through topological transitions (Weaire & Rivier, 1984; Weaire & Fortes, 1994), leading to irreversible plastic deformations of the tissue. Preliminary studies of a 2D version of this model suggest that the cells on the outer surface of an aggregate may adopt a significantly different shape to those in the interior. Such discrete effects may require consideration of a hybrid model, in which a continuum approximation in the interior is matched with a discrete solution valid near the edge.

In summary, when the number of cells in the IBM is large, we may approximate its behaviour with a continuum model. When the parameters of cells vary slowly in space, the approximation is valid if the cell pressures and vertex velocities vary spatially over many cells; for spatially periodic cell properties, we require that variation in mean pressures and velocities occurs on a scale which is much larger than the periodic unit. While we do not give *a priori* restrictions on the model parameters for these assumptions to hold, for any particular simulation these conditions can be verified from the (numerical) solution of the continuum approximation.

This analysis shows how convective derivatives arise naturally in continuum models of cell populations, even though they have been neglected in many previous models. It also puts other models on a stronger theoretical foundation by connecting continuum models with the mechanical properties of individual cells.

Acknowledgement

We thank the anonymous referees for their helpful comments.

Funding

Biotechnology and Biological Sciences Research Council (BBD0085221).

REFERENCES

ALARCÓN, T., BYRNE, H. M. & MAINI, P. K. (2004) Towards whole-organ modelling of tumour growth. *Prog. Biophys. Mol. Biol.*, **85**, 451–472.

ALBER, M., CHEN, N., LUSHNIKOV, P. M. & NEWMAN, S. A. (2007) Continuous macroscopic limit of a discrete stochastic model for interaction of living cells. *Phys. Rev. Lett.*, **99**, 168102.

ALBERTS, B., JOHNSON, A., LEWIS, J., RAFF, M., ROBERTS, K. & WALTER, P. (2008) *Molecular Biology of the Cell*. New York: Garland Science.

ALBEVERIO, S. & ALT, W. (2008) Stochastic dynamics of viscoelastic skeins: condensation waves and continuum limits, *Math. Models Methods Appl. Sci.*, **18**, 1149–1191.

ALT, W. (2002) Nonlinear hyperbolic systems of generalized Navier-Stokes type for interactive motion in biology. *Geometric Analysis and Nonlinear Partial Differential Equations* (S. Hildebrandt & H. Karcher eds). Heidelberg: Springer, pp. 431–461.

ANDERSON, A. R. A. (2007) A hybrid multiscale model of tumour invasion: evolution and the microenvironment. *Single-cell-based Models in Biology and Medicine, Mathematics and Biosciences in Interaction* (A. Anderson, M. Chaplain & K. Rejniak eds), chapter I.1. Basel: Birkhäuser, pp. 3–28.

ANDERSON, A. R. A. & QUARANTA, V. (2008) Integrative mathematical oncology. *Nat. Rev. Cancer*, **8**, 227–234.

ARAUJO, R. P. & MCELWAIN, D. L. S. (2002) A history of the study of solid tumour growth: the contribution of mathematical modelling, *Bull. Math. Biol.*, **66**, 1039–1091.

BARENBLATT, G. I., ZHELTOV, I. P. & KOCHINA, I. N. (1960) Basic concepts in the theory of seepage of homogeneous liquids in fissured rocks (strata). *J. Appl. Math. Mech.*, **24**, 1286–1303.

BENSOUSSAN, A., LIONS, J. L. & PAPANICOLAOU, G. (1978) *Asymptotic Analysis for Periodic Structures*. Amsterdam: North Holland.

BINDSCHADLER, M. & MCGRATH, J. L. (2007) Sheet migration by wounded monolayers as an emergent property of single-cell dynamics. *J. Cell Sci.*, **120**, 876–884.

BODNAR, M. & VELAZQUEZ, J. J. L (2005) Derivation of macroscopic equations for individual cell-based models: a formal approach. *Math. Models Methods Appl. Sci.*, **28**, 1757–1779.

BRESSLOFF, P. C. (2001). Travelling fronts and wave propagation failure in an inhomogeneous neural network. *Phys. D*, **155**, 83–100.

BRODLAND, G. W. (2004) Computational modeling of cell sorting, tissue engulfment, and related phenomena: a review. *Appl. Mech. Rev.*, **57**, 47–76.

BYRNE, H. M. & CHAPLAIN, M. A. J. (1996) Modelling the role of cell-cell adhesion in the growth and development of carcinomas. *Math. Comput. Model.*, **24**, 1–17.

CETIN, S., LEAPHART, C. L., LI, J., ISCHENKO, I., HAYMAN, M., UPPERMAN, J., ZAMORA, R., WATKINS, S., FORD, H. R., WANG, J. & HACKAM, D. J. (2007) Nitric oxide inhibits enterocyte migration through activation of RhoA-GTPase in a SHP-2 dependent manner. *Am. J. Physiol. Gatrointest. Liver Physiol.*, **292**, G1347–G1358.

CHEN, H. H. & BRODLAND, G. W. (2000) Cell-level finite-element studies of viscous cells in planar aggregates. *J. Biomech. Eng.*, **122**, 394–401.

CHILDRESS, S. & PERCUS, J. P. (1981) Modeling of cell and tissue movements in the developing embryo. *Lect Math Life Sci.*, **14**, 59–88.

CORKINS, M. R., PARK, J. H. Y, DAVIS, D. V., SLENTZ, D. H. & MACDONALD, R. G. (1999) Regulation of the insulin-like growth factor axis by increasing cell number in intestinal epithelial (IEC-6) cells. *Growth Horm. IGF Res.*, **9**, 414–424.

DE MASI, A., LUCKHAUS, S. & PRESUTTI, E. (2007) Two scales hydrodynamic limit for a model of malignant tumour cells. *Ann. Inst. H. Poincaré Probab. Statist.*, **43**, 257–297.

DRASDO, D. (2005) Coarse graining in simulated cell populations. *Adv. Complex Syst.*, **8**, 319–363.

DU ROURE, O., SAEZ, A., BUGUIN, A., AUSTIN, R. H., CHAVRIER, P., SIBERZAN, P. & LADOUX, B. (2005) Force mapping in epithelial cell migration. *Proc. Natl. Acad. Sci. USA*, **102**, 2390–2395.

EDWARDS, C. M. & CHAPMAN, S. J. (2007). Biomechanical modelling of colorectal crypt budding and fission. *Bull. Math. Biol.*, **69**, 1927–1942.

FAROOQUI, R. & FENTEANY, G. (2005) Multiple rows of cells behind an epithelial wound edge extend cryptic lamellipodia to collectively drive cell-sheet movement. *J. Cell Sci.*, **118**, 51–63.

GALLE, J., LOEFFLER, M. & DRASDO, D. (2005) Modeling the effect of deregulated proliferation and apoptosis on the growth dynamics of epithelial cell populations in vitro. *Biophys. J.*, **88**, 62–75.

GLAZIER, J. A., BALTER, A. & POPLAWSKI, N. J. (2007) Magnetization to morphogenesis: A brief history of the Glazier-Graner-Hogeweg model. *Single-Cell-Based Models in Biology and Medicine, Mathematics and Biosciences in Interaction* (A. Anderson, M. Chaplain & K. Rejniak eds), chapter II.1. Basel: Birkhäuser, pp. 79–106.

GOEL, P., SNEYD, J. & FRIEDMAN, A. (2006) Homogenization of the cell cytoplasm: the calcium bidomain equations. *Multiscale Model. Simul.*, **5**, 1045–1062.

GRANER, F. & GLAZIER, J. A. (1992) Simulation of biological cell sorting using a two-dimensional extended Potts model. *Phys. Rev. Lett.*, **69**, 2013–2016.

GREENSPAN, H. P. (1976) On the growth and stability of cell cultures and solid tumors. *J. Theor. Biol.*, **56**, 229–242.

HAGA, H., IRAHARA, C., KOBAYSHI, R., NAKAGAKI, T. & KAWABATA, K. (2005) Collective movement of epithelial cells on a collagen gel substrate. *Biophys. J.*, **88**, 2250–2256.

HILGENFELDT, S., ERIKSEN, S. & CARTHEW, R. W. (2008) Physical modeling of cell geometric order in an epithelial tissue. *Proc. Natl Acad. Sci. USA*, **105**, 907–911.

HOGEWEG, P. (2000) Evolving mechanisms of morphogenesis: on the interplay between differential adhesion and cell differentiation. *J. Theor. Biol.*, **203**, 317–333.

HORNUNG, U. (ed.) (1997) *Homogenization and Porous Media*. Heidelberg: Springer.

HUMPHRIES, A. & WRIGHT, N. A. (2008) Colonic crypt organization and tumorigenesis. *Nat. Rev. Cancer*, **8**, 415–424.

KECK, J. & CARRIER, G. (1965) Diffusion theory of nonequilibrium dissociation and recombination. *J. Chem. Phys.*, **43**, 2284–2298.

KEENER, J. P. (2000) Homogenization and propagation in the bistable equation. *Phys. D*, **136**, 1–17.

KEVREKIDIS, P. G., KEVREKIDIS, I. G., BISHOP, A. R. & TITI, E. S. (2002) Continuum approach to discreteness. *Phys. Rev. E.*, **65**, 046613.

KLEIN, T. J. & MLODZIK, M. (2005) Planar cell polarization: an emerging model points in the right direction. *Annu. Rev. Cell Dev. Biol.*, **21**, 155–176.

KRUSKAL, M. D. & ZABUSKY, N. J. (1964) Stroboscopic-perturbation procedure for treating a class of nonlinear wave equations. *J. Math. Phys.*, **5**, 231–244.

LEMON, G., KING, J. R., BYRNE, H. M., JENSEN, O. E. & SHAKESHEFF, K. (2006) Multiphase modelling of tissue growth using the theory of mixtures. *J. Math. Biol.*, **52**, 571–594.

LUSHNIKOV, P. M., CHEN, N. & ALBER, M. (2008) Macroscopic dynamics of biological cells interacting via chemotaxis and direct contact. *Phys. Rev. E*, **78**, 061904.

MARÉE, A. F. M., JILKINE, A., DAWES, A., GRIENEISEN, V. A. & EDELSTEIN-KESHET, L. (2006) Polarization and movement of keratocytes: a multiscale modelling approach. *Bull. Math. Biol.*, **68**, 1169–1211.

MARTIN, P. (1997). Wound healing–aiming for perfect skin regeneration. *Science*, **276**, 75–81.

MEINEKE, F. A., POTTEN, C. S. & LOEFFLER, M. (2001) Cell migration and organization in the intestinal crypt using a lattice-free model. *Cell Prolif.*, **34**, 253–266.

MERKS, R. M. H. & GLAZIER, J. A. (2005) A cell-centered approach to developmental biology. *Phys. A*, **352**, 113–130.

MI, Q., SWIGON, D., RIVIÈRE, B., CETIN, S., VODOVOTZ, Y. & HACKAM, D. J. (2007) One-dimensional elastic continuum model of enterocyte layer migration. *Biophys. J.*, **93**, 3745–3752.

MILTON, G. W. (2002) *The Theory of Composites*. Cambridge: CUP.

MURRAY, J. D. & OSTER, G. F. (1984) Generation of biological pattern and form. *IMA J. Math. Appl. Med. Biol.*, **1**, 51–75.

NAGAI, T. & HONDA, H. (2001) A dynamic cell model for the formation of epithelial tissues. *Phil. Mag. B*, **81**, 699–719.

NEWMAN, T. J. & GRIMA, R. (2004) Many-body theory of chemotactic cell-cell interactions. *Phys. Rev. E*, **70**, 051916.

NOVÁK, B. & TYSON, J. J. (2004) A model for restriction point control of the mammalian cell cycle. *J. Theor. Biol.*, **230**, 563–579.

ODELL, G. M., OSTER, G., ALBERCH, P. & BURNSIDE, B. (1981) The mechanical basis of morphogenesis. I. Epithelial folding and invagination. *Dev. Biol.*, **85**, 446–462.

OLSEN, L., SHERRATT, J. A. & MAINI, P. K. (1995) A mechanichemical model for adult dermal wound contraction: on the permanence of the contracted tissue displacement profile. *J. Theor. Biol.*, **177**, 113–128.

OTHMER, H. G. (1983) A continuum model for coupled cells. *J. Math. Biol.*, **17**, 351–369.

OWEN, M. R., SHERRATT, J. A. & WEARING, H. J. (2000) Lateral induction by juxtacrine signaling is a new mechanism for pattern formation. *Dev. Biol.*, **217**, 54–61.

PAVLIOTIS, G. A. & STUART, A. M. (2008) *Multiscale Methods: Averaging and Homogenization*. Heidelberg: Springer.

POUJADE, M., GRASLAND-MONGRAIN, E., HERTZOG, A., JOUANNEAU, J., CHAVRIER, P., LADOUX, B., BUGUIN, A. & SILBERZAN, P. (2007) Collective migration of an epithelial monolayer in response to a model wound. *Proc. Natl. Acad. Sci. USA*, **104**, 15988–15993.

PRASS, M., JACOBSON, K., MOGILNER, A. & RADMACHER, M. (2006) Direct measurement of the lamellipodial protrusive force in a migrating cell. *J. Cell. Biol.*, **174**, 767–772.

QUARONI, A., WANDS, J., TRELSTAD, R. L. & ISSELBACHER, K. J. (1979) Epithelioid cell cultures from rat small intestine. Characterization by morphologic and immunologic criteria. *J. Cell. Biol.*, **80**, 248–265.

RAMIS-CONDE, I., DRASDO, D. ANDERSON, A. R. A. & CHAPLAIN, M. A. J. (2008) Modeling the influence of the E-cadherin-β-catenin pathway in cancer cell invasion: a multiscale approach. *Biophys. J.*, **95**, 155–165.

REINHART-KING, C. A., DEMBO, M. & HAMMER, D. A. (2005) The dynamics and mechanics of endothelial cell spreading. *Biophys. J.*, **89**, 676–689.

RODRIGUEZ, E. K., HOGER, A. & MCCULLOCH, A. D. (1994) Stress-dependent finite growth in soft elastic tissues. *J. Biomech.*, **27**, 455–467.

ROOSE, T., CHAPMAN, S. J. & MAINI, P. K. (2007) Mathematical models of avascular tumor growth. *SIAM Rev.*, **49**, 179–208.

ROSEN, P. & MISFELDT, D. S. (1980) Cell density determines epithelial migration in culture *Proc. Natl. Acad. Sci. USA*, **77**, 4760–4763.

SAVILL, N. J. & SHERRATT, J. A. (2003) Control of epidermal stem cell clusters by Notch-mediated lateral induction. *Dev. Biol.*, **258**, 141–153.

SCHÖCK, F. & PERRIMON, N. (2002) Molecular mechanisms of epithelial morphogenesis. *Annu. Rev. Cell Dev. Biol.*, **18**, 463–93.

SHERRATT, J. A. & MURRAY, J. D. (1990) Models of epidermal wound healing. *Proc. R. Soc. Lond. B*, **241**, 29–36.

STEVENS, A. (2000) The derivation of chemotaxis equations as limit dynamics of moderately interacting stochastic many-particle systems. *SIAM J. Appl. Math.*, **61**, 183–212.

THOUMINE, O. & OTT, A. (1997) Time scale dependent viscoelastic and contractile regimes in fibroblasts probed by microplate manipulation. *J. Cell. Sci.*, **110**, 2109–2116.

TING, T. W. (1963) Certain non-steady flows of second-order fluids. *Arch. Rat. Mech. Anal.*, **14**, 1–26.

TRANQUILLO, R. T. & MURRAY, J. D. (1992) Continuum model of fibroblast-driven wound contraction: inflammation-mediation. *J. Theor. Biol.*, **158**, 135–172.

TREFETHEN, L. N. (2000) *Spectral Methods in MATLAB*. Philadelphia, PA: SIAM.

TURNER, S., SHERRATT, J. A., PAINTER, K. J. & SAVILL, N. J. (2004). From a discrete to a continuous model of biological cell movement. *Phys. Rev. E*, **69**, 021910.

VAN LEEUWEN, I. M. M., MIRAMS, G. R., WALTER, A., FLETCHER, A., MURRAY, P., OSBORNE, J., VARMA, S., YOUNG, S. J., COOPER, J., PITT-FRANCIS, J., MOMTAHAN, L., PATHMANATHAN, P., WHITELEY, J. P., CHAPMAN, S. J., GAVAGHAN, D. J., JENSEN, O. E., KING, J. R., MAINI, P. K., WATERS, S. L. & BYRNE, H. M. (2009) An integrative computational model for intestinal tissue renewal. *Cell Prolif.*, **45**, 617–636.

WALKER, D. C., HILL, G., WOOD, S. M., SMALLWOOD, R. H. & SOUTHGATE, J. (2004) Agent-based computational modeling of wounded epithelial cell monolayers. *IEEE Trans. Nanobiosci.*, **3**, 153–163.

WEAIRE, D. & FORTES, M. A. (1994) Stress and strain in liquid and solid foams. *Adv. Phys.*, **43**, 685–738.

WEAIRE, D. & RIVIER, N. (1984) Soap, cells and statistics–random patterns in two dimensions. *Contemp. Phys.*, **25**, 59–99.

WELIKY, M. & OSTER, G. (1990) The mechanical basis of cell rearrangement. I. Epithelial morphogenesis during Fundulus epiboly. *Development*, **109**, 373–386.

ZABUSKY, N. J. & KRUSKAL, M. D. (1965) Interactions of "solitons" in a collisionless plasma and the recurrence of initial states. *Phys. Rev. Lett.*, **15**, 240–243.

Appendix A. Variational formulation of the slowly varying approximation

The slowly varying continuum approximation (3.2) may also be derived directly from the energy-gradient formulation (through a similar procedure to that of Childress & Percus, 1981), and the IBM may be identified with a particular (mixed Galerkin) finite-element discretization of the continuum approximation.

We introduce the finite-dimensional spaces $S_N \subset L^2([0, N])$, which consists of the functions that are constant on each subinterval $(n, n+1)$ for all $n = 0, \ldots, N-1$, and $V_N \subset H^1([0, N])$, which consists of the continuous functions that are linear on each subinterval $(n, n+1)$. The space S_N has a basis of piecewise constant functions

$$\psi_{n+1/2}(\nu) = \begin{cases} 1, & \nu \in (n, n+1), \\ 0, & \text{elsewhere}, \end{cases} \qquad n = 0, \ldots, N-1,$$

and V_N has a basis of linear hat functions

$$\chi_n(\nu) = \begin{cases} \nu - n + 1, & \nu \in [n-1, n), \\ n + 1 - \nu, & \nu \in [n, n+1), \\ 0, & \text{elsewhere}, \end{cases} \qquad n = 0, \ldots, N.$$

On extending all cell-based quantities and parameters to functions in S_N through

$$\phi^d(\nu, t) = \sum_{n=0}^{N-1} \phi_{n+1/2}(t)\psi_{n+1/2}(\nu),$$

and the vertex velocities to a function in V_N,

$$u^d(\nu, t) = \sum_{n=0}^{N} u_n(t)\chi_n(\nu),$$

the free energy and dissipation rate for the IBM can be written (exactly) as

$$H = \int_0^N \frac{\lambda^d}{2}(a^d - l^d)^2 \,\mathrm{d}\nu, \quad \Phi = \int_0^N \left\{ \mu^d l^d (u^d)^2 + V\delta^d \left(\frac{\partial u^d}{\partial \nu} \right)^2 \right\} \mathrm{d}\nu. \tag{A.1}$$

Equations (2.16a) and (2.16c) of the IBM are identical to

$$(\mu^d l^d u^d, \chi_n) + V\left(\delta^d \frac{\partial u^d}{\partial \nu}, \frac{\mathrm{d}\chi_n}{\mathrm{d}\nu}\right) = \left(p^d, \frac{\mathrm{d}\chi_n}{\mathrm{d}\nu}\right), \quad n = 0, \ldots, N,$$

$$\left(\frac{\partial l^d}{\partial t}, \psi_{n+1/2}\right) = \left(\frac{\partial u^d}{\partial \nu}, \psi_{n+1/2}\right), \quad n = 0, \ldots, N-1,$$

where $(\cdot, \cdot)$ denotes the inner product on $L^2([0, N])$, given by

$$(f, g) = \int_0^N f(\nu)g(\nu) \,\mathrm{d}\nu.$$

On scaling all variables according to (3.1), these are the Galerkin equations for the weak forms

$$(\mu l\tilde{u}, \chi) + \tilde{V}\left(\delta\frac{\partial\tilde{u}}{\partial\tilde{\nu}}, \frac{\mathrm{d}\chi}{\mathrm{d}\tilde{\nu}}\right) = \left(\tilde{p}, \frac{\mathrm{d}\chi}{\mathrm{d}\tilde{\nu}}\right), \quad \forall\,\chi \in H^1([0,1]), \tag{A.2a}$$

$$\left(\frac{\partial l}{\partial\tilde{t}}, \psi\right) = \left(\frac{\partial\tilde{u}}{\partial\tilde{\nu}}, \psi\right), \quad \forall\,\psi \in L^2([0,1]), \tag{A.2b}$$

of the slowly varying equations (3.2a) and (3.2c) with boundary conditions (3.3). Alternatively, we may arrive at (A.2) by first replacing all the approximate functions in (A.1) by their continuum counterparts, rescaling all quantities following (3.1) and applying the variational principle used for the IBM (maximum rate of decrease in the free energy); the boundary conditions (3.3) are the natural conditions arising for this variational problem.

We will not consider the convergence of this scheme in any rigorous detail, but note that the accuracy of the approximation requires that the solutions of the continuum models be well approximated in the finite-dimensional subspaces (S_N and V_N), which corresponds to the slowly varying assumption. A higher-order version of this discretization (with a piecewise linear discretization for the pressure, piecewise quadratic velocities and with the rescaled domain $\tilde{\nu} \in [0,1]$ divided into a number of intervals which differs from the number of cells in the IBM) was used for numerical simulation of the continuum approximations.

Appendix B. Continuum approximation with heterogeneous cell parameters

Here we restrict attention to problems with periodic cell properties (with period $M = O(1)$) and examine the behaviour of the system for large total cell number N. We consider the discrete system (2.16), with the growth rate constant for each cell ($\Gamma(l, p, a; \gamma) \equiv \gamma$). As in the slowly varying approximation, we expect that the leading-order pressure and velocities will vary over $N \gg 1$ cells, and introduce the scalings (3.1). Following the usual multiple scales philosophy, we write

$$\tilde{p}_{n+1/2} \equiv \tilde{p}(n+\tfrac{1}{2}, \tilde{\nu}+\tfrac{1}{2N}, \tilde{t}), \quad l_{n+1/2} \equiv l(n+\tfrac{1}{2}, \tilde{\nu}+\tfrac{1}{2N}, \tilde{t}), \quad \tilde{u}_n \equiv \tilde{u}(n, \tilde{\nu}, \tilde{t}),$$

where n and $\tilde{\nu}$ are treated as as independent variables, and we require that $\tilde{p}$, l and $\tilde{u}$ are M-periodic functions of n for each fixed value of $\tilde{\nu}$. We differ from the standard analysis by only allowing n to take integer values, while $\tilde{\nu}$ is a continuous variable. The finite differences in (2.16a) and (2.16c) are replaced by

$$\begin{aligned}
\tilde{p}_{n-1/2} - \tilde{p}_{n+1/2} &\equiv \tilde{p}(n-\tfrac{1}{2}, \tilde{\nu}-\tfrac{1}{2N}, \tilde{t}) - \tilde{p}(n+\tfrac{1}{2}, \tilde{\nu}+\tfrac{1}{2N}, \tilde{t}) \\
&= \tilde{p}(n-\tfrac{1}{2}, \tilde{\nu}, \tilde{t}) - \tilde{p}(n+\tfrac{1}{2}, \tilde{\nu}, \tilde{t}) \\
&\qquad - \frac{1}{2N}\left(\frac{\partial\tilde{p}}{\partial\tilde{\nu}}(n-\tfrac{1}{2}, \tilde{\nu}, \tilde{t}) + \frac{\partial\tilde{p}}{\partial\tilde{\nu}}(n+\tfrac{1}{2}, \tilde{\nu}, \tilde{t})\right) + O(N^{-2}), \\
\tilde{u}_{n+1} - \tilde{u}_n &\equiv \tilde{u}(n+1, \tilde{\nu}+\tfrac{1}{N}, \tilde{t}) - \tilde{u}(n, \tilde{\nu}, \tilde{t}) \\
&= \tilde{u}(n+1, \tilde{\nu}+\tfrac{1}{2N}, \tilde{t}) - \tilde{u}(n, \tilde{\nu}+\tfrac{1}{2N}, \tilde{t}) \\
&\qquad + \frac{1}{2N}\left(\frac{\partial\tilde{u}}{\partial\tilde{\nu}}(n+1, \tilde{\nu}+\tfrac{1}{2N}, \tilde{t}) + \frac{\partial\tilde{u}}{\partial\tilde{\nu}}(n, \tilde{\nu}+\tfrac{1}{2N}, \tilde{t})\right) + O(N^{-2}),
\end{aligned}$$

and the vertex velocities in (2.16a) are expanded as

$$\tilde{u}_{n+1} \equiv \tilde{u}(n+1, \tilde{\nu} + \tfrac{1}{N}, \tilde{t}) = \tilde{u}(n+1, \tilde{\nu}, \tilde{t}) + \frac{1}{N}\frac{\partial \tilde{u}}{\partial \tilde{\nu}}(n+1, \tilde{\nu}, \tilde{t}) + \frac{1}{2N^2}\frac{\partial^2 \tilde{u}}{\partial \tilde{\nu}^2}(n+1, \tilde{\nu}, \tilde{t}) + O(N^{-3}),$$

$$\tilde{u}_{n-1} \equiv \tilde{u}(n-1, \tilde{\nu} - \tfrac{1}{N}, \tilde{t}) = \tilde{u}(n-1, \tilde{\nu}, \tilde{t}) - \frac{1}{N}\frac{\partial \tilde{u}}{\partial \tilde{\nu}}(n-1, \tilde{\nu}, \tilde{t}) + \frac{1}{2N^2}\frac{\partial^2 \tilde{u}}{\partial \tilde{\nu}^2}(n-1, \tilde{\nu}, \tilde{t}) + O(N^{-3}).$$

The somewhat unusual form of these expansions comes from a desire to write the differences in a symmetric form, with all quantities in each equation being evaluated at the same value of $\tilde{\nu}$. We seek asymptotic expansions of the solutions of the form

$$\tilde{p} \sim \tilde{p}^{(0)} + \frac{1}{N}\tilde{p}^{(1)} + \ldots, \quad \tilde{u} \sim \tilde{u}^{(0)} + \frac{1}{N}\tilde{u}^{(1)} + \ldots, \qquad l \sim l^{(0)} + \frac{1}{N}l^{(1)} + \ldots.$$

We consider situations without (B.1) and with (B.2) cell viscosity below.

B.1 *No cell viscosity ($\tilde{V} = 0$)*

B.1.1 *Short-scale variations.*

At leading order, (2.16a) gives

$$\tilde{p}^{(0)}(n - \tfrac{1}{2}, \tilde{\nu}, \tilde{t}) - \tilde{p}^{(0)}(n + \tfrac{1}{2}, \tilde{\nu}, \tilde{t}) = 0,$$

for all $\tilde{\nu} \in [0, 1]$, and as $\tilde{p}^{(0)}$ is periodic in the discrete variable n, we have that $\tilde{p}^{(0)} \equiv \tilde{p}^{(0)}(\tilde{\nu}, \tilde{t})$ (i.e. the leading-order cell pressures depend on the cell index only through the continuous variable $\tilde{\nu}$.)

The leading-order terms in (2.16c) are

$$\tilde{u}^{(0)}(n+1, \tilde{\nu} + \tfrac{1}{2N}, \tilde{t}) - \tilde{u}^{(0)}(n, \tilde{\nu} + \tfrac{1}{2N}, \tilde{t}) = 0,$$

so (as for $\tilde{p}^{(0)}$) $\tilde{u}^{(0)} \equiv \tilde{u}^{(0)}(\tilde{\nu}, \tilde{t})$. At $O(1/N)$, (2.16a) gives

$$\frac{1}{2}\left\{\mu_{n-1/2}l^{(0)}(n - \tfrac{1}{2}, \tilde{\nu}, \tilde{t}) + \mu_{n+1/2}l^{(0)}(n + \tfrac{1}{2}, \tilde{\nu}, \tilde{t})\right\}\tilde{u}^{(0)}(\tilde{\nu}, \tilde{t}) + \frac{\partial \tilde{p}^{(0)}}{\partial \tilde{\nu}}(\tilde{\nu}, \tilde{t})$$
$$= \tilde{p}^{(1)}(n - \tfrac{1}{2}, \tilde{\nu}, \tilde{t}) - \tilde{p}^{(1)}(n + \tfrac{1}{2}, \tilde{\nu}, \tilde{t}) \quad \text{(B.1)}$$

for all $\tilde{\nu} \in [0, 1]$, where

$$l^{(0)}(n + \tfrac{1}{2}, \tilde{\nu}, \tilde{t}) = a_{n+1/2}(\tilde{t}) - \frac{1}{\lambda_{n+1/2}}\tilde{p}^{(0)}(\tilde{\nu}, \tilde{t}). \quad \text{(B.2)}$$

Periodicity of $\tilde{p}^{(1)}$ requires that

$$\overline{\mu_{n+1/2}l^{(0)}(n + \tfrac{1}{2}, \tilde{\nu}, \tilde{t})}\tilde{u}^{(0)}(\tilde{\nu}, \tilde{t}) = -\frac{\partial \tilde{p}^{(0)}}{\partial \tilde{\nu}}(\tilde{\nu}, \tilde{t}), \quad \text{(B.3)}$$

where the over-line denotes the average value of a quantity, with respect to the discrete cell index n, over one period of M cells. If $\mu_{n+1/2}$ is not correlated with $a_{n+1/2}$ or $1/\lambda_{n+1/2}$ (i.e. $\overline{\mu a} = \bar{\mu}\bar{a}$, $\overline{\mu/\lambda} = \bar{\mu}\overline{(1/\lambda)}$), then $\overline{\mu l^{(0)}}(\tilde{\nu}, \tilde{t}) = \bar{\mu}\overline{l^{(0)}}(\tilde{\nu}, \tilde{t})$ and (B.3) becomes

$$\bar{\mu}\overline{l^{(0)}}(\tilde{\nu}, \tilde{t})\tilde{u}^{(0)}(\tilde{\nu}, \tilde{t}) = -\frac{\partial \tilde{p}^{(0)}}{\partial \tilde{\nu}}(\tilde{\nu}, \tilde{t}). \quad \text{(B.4)}$$

Observe that (B.4) relates the leading-order vertex velocities and cell pressures and is equivalent to (3.2a) in the slowly varying approximation, with all parameters replaced by their cell-based averages, the cell pressures and vertex velocities replaced by their slowly varying parts, and the cell lengths replaced by their average values over a period. Taking the average of (B.2), we have

$$\overline{l^{(0)}}(\tilde{\nu},\tilde{t}) = \bar{a}(\tilde{t}) - \overline{(1/\lambda)}\tilde{p}^{(0)}(\tilde{\nu},\tilde{t}), \tag{B.5}$$

which has the same form as (3.2b), but with λ now replaced by $1/\overline{(1/\lambda)}$.

B.1.2 *Large-scale variations.* At $O(1/N^2)$, (2.16c) becomes

$$\frac{\partial l^{(0)}}{\partial \tilde{t}}(n+\tfrac{1}{2},\tilde{\nu}+\tfrac{1}{2N},\tilde{t}) - \frac{\partial \tilde{u}^{(0)}}{\partial \tilde{\nu}}(\tilde{\nu}+\tfrac{1}{2N},\tilde{t}) = \tilde{u}^{(1)}(n+1,\tilde{\nu}+\tfrac{1}{2N},\tilde{t}) - \tilde{u}^{(1)}(n,\tilde{\nu}+\tfrac{1}{2N},\tilde{t}). \tag{B.6}$$

Again, in order for $\tilde{u}^{(1)}$ to have a periodic solution, we require that the average of the left-hand side over the period vanishes; this condition becomes

$$\frac{\partial \overline{l^{(0)}}}{\partial t}(\tilde{\nu}+\tfrac{1}{2N},\tilde{t}) = \frac{\partial \tilde{u}^{(0)}}{\partial \nu}(\tilde{\nu}+\tfrac{1}{2N},\tilde{t}), \tag{B.7}$$

which is equivalent to (3.2c).

Taking the average of (2.16d) over a period, we find that

$$\frac{\partial \bar{a}}{\partial \tilde{t}} = \tilde{\alpha}\bar{\gamma}, \tag{B.8}$$

which is equivalent to (3.2d).

At leading order, the (2.18) for the end vertices become

$$\tilde{p}^{(0)}(0,\tilde{t}) = 0, \quad \tilde{p}^{(0)}(1,\tilde{t}) = 0,$$

which are the same as the boundary conditions (3.3) for the slowly varying approximation when $\tilde{V} = 0$.

In summary, we find that the leading-order cell pressures and vertex velocities depend on the cell index only through the large length-scale variable $\tilde{\nu}$; these (along with the mean cell lengths) satisfy the system of equations (B.4), (B.5), (B.7) and (B.8), which are the analogue of (3.2), but with all parameters replaced by their appropriate average values.

B.2 *With cell viscosity*

In order for the cell viscosity terms to affect the leading-order equations, we require (as in the slowly varying approximation) that $\tilde{V} \equiv V/N^2 = O(1)$ as $N \to \infty$.

B.2.1 *Short-scale variations.* While (2.16c) still gives us that $\tilde{u}^{(0)} \equiv \tilde{u}^{(0)}(\tilde{\nu},\tilde{t})$, it is helpful to rewrite (2.16a) as

$$\frac{\mu_{n-1/2}l_{n-1/2}(u_{n-1}+2u_n)}{6} + \frac{\mu_{n+1/2}l_{n+1/2}(2u_n+u_{n+1})}{6} - V\left(\delta_{n+1/2}\frac{\mathrm{d}l_{n+1/2}}{\mathrm{d}t} - \delta_{n-1/2}\frac{\mathrm{d}l_{n-1/2}}{\mathrm{d}t}\right) = p_{n-1/2} - p_{n+1/2}, \tag{B.9}$$

which, on scaling all variables following (3.1), introducing the multiple scales ansatz, and expanding all variables in powers of $1/N$, has $O(1)$ contribution

$$-\tilde{V}\left\{\delta_{n+1/2}\frac{\partial l^{(0)}}{\partial \tilde{t}}(n+\tfrac{1}{2},\tilde{\nu},\tilde{t})-\delta_{n-1/2}\frac{\partial l^{(0)}}{\partial \tilde{t}}(n-\tfrac{1}{2},\tilde{\nu},\tilde{t})\right\}=\tilde{p}^{(0)}(n-\tfrac{1}{2},\tilde{\nu},\tilde{t})-\tilde{p}^{(0)}(n+\tfrac{1}{2},\tilde{\nu},\tilde{t}).$$

The condition for this to have solutions for $l^{(0)}$ and $\tilde{p}^{(0)}$ which are periodic in n is

$$\tilde{p}^{(0)}(n+\tfrac{1}{2},\tilde{\nu},\tilde{t})-\tilde{V}\delta_{n+1/2}\frac{\partial l^{(0)}}{\partial \tilde{t}}(n+\tfrac{1}{2},\tilde{\nu},\tilde{t})=A^{(0)}(\tilde{\nu},\tilde{t}), \tag{B.10}$$

for some function $A^{(0)}(\tilde{\nu},\tilde{t})$; we note that the left-hand side of (B.10) is the total force exerted by a cell on its neighbours (not including cell–substrate drag forces). We also have from (2.16b) that

$$l^{(0)}(n+\tfrac{1}{2},\tilde{\nu},\tilde{t})=a_{n+1/2}(\tilde{t})-\frac{\tilde{p}^{(0)}(n+\frac{1}{2},\tilde{\nu},\tilde{t})}{\lambda_{n+1/2}}, \tag{B.11}$$

and so (B.10), (B.11) and (2.16d) give us the differential equations

$$\tilde{p}^{(0)}(n+\frac{1}{2},\tilde{\nu},\tilde{t})-\tilde{V}\delta_{n+1/2}\left(\tilde{\alpha}\gamma_{n+1/2}-\frac{1}{\lambda_{n+1/2}}\frac{\partial \tilde{p}^{(0)}}{\partial \tilde{t}}(n+\frac{1}{2},\tilde{\nu},\tilde{t})\right)=A^{(0)}(\tilde{\nu},\tilde{t}), \tag{B.12}$$

for $n=0,\ldots,M-1$. Taking the average of (B.10) over a period we have that

$$A^{(0)}(\tilde{\nu},\tilde{t})=\overline{\tilde{p}^{(0)}}(\tilde{\nu},\tilde{t})-\overline{\tilde{V}\delta_{n+1/2}\frac{\partial l^{(0)}}{\partial \tilde{t}}(n+\tfrac{1}{2},\tilde{\nu},\tilde{t})}, \tag{B.13}$$

or alternatively

$$\overline{\left(\frac{1}{\tilde{V}\delta_{n+1/2}}\right)}A^{(0)}(\tilde{\nu},\tilde{t})=\overline{\left(\frac{\tilde{p}^{(0)}(n+\frac{1}{2},\tilde{\nu},\tilde{t})}{\tilde{V}\delta_{n+1/2}}\right)}-\frac{\partial\overline{l^{(0)}}}{\partial \tilde{t}}(\tilde{\nu},\tilde{t}). \tag{B.14}$$

Taking the average of (B.2), we have that

$$\overline{l^{(0)}}(\tilde{\nu},\tilde{t})=\bar{a}(\tilde{t})-\overline{\left(\frac{\tilde{p}^{(0)}(n+\frac{1}{2},\tilde{\nu},\tilde{t})}{\lambda_{n+1/2}}\right)}.$$

We expect from (B.12) that $\tilde{p}^{(0)}(n+\frac{1}{2},\tilde{\nu},\tilde{t})$ and $l^{(0)}(n+\frac{1}{2},\tilde{\nu},\tilde{t})$ will be correlated with $\lambda_{n+1/2}$, $\delta_{n+1/2}$ and $\gamma_{n+1/2}$.

B.2.2 *Large-scale variations.* As for the case where $\tilde{V}=0$, (B.6) still holds, so we again recover (B.7) from the solvability condition; (B.8) also holds in this case.

The $O(1/N)$ contribution to (B.9) is

$$\frac{1}{2}\left(\mu_{n-1/2}l^{(0)}(n-\tfrac{1}{2},\tilde{\nu},\tilde{t})+\mu_{n+1/2}l^{(0)}(n+\tfrac{1}{2},\tilde{\nu},\tilde{t})\right)\tilde{u}^{(0)}(\tilde{\nu},\tilde{t})$$
$$-\tilde{V}\left\{\delta_{n+1/2}\frac{\partial l^{(1)}}{\partial\tilde{t}}(n+\tfrac{1}{2},\tilde{\nu},\tilde{t})-\delta_{n-1/2}\frac{\partial l^{(1)}}{\partial\tilde{t}}(n-\tfrac{1}{2},\tilde{\nu},\tilde{t})\right.$$
$$\left.+\frac{1}{2}\left(\delta_{n+1/2}\frac{\partial^2 l^{(0)}}{\partial\tilde{t}\partial\tilde{\nu}}(n+\tfrac{1}{2},\tilde{\nu},\tilde{t})+\delta_{n-1/2}\frac{\partial^2 l^{(0)}}{\partial\tilde{t}\partial\tilde{\nu}}(n-\tfrac{1}{2},\tilde{\nu},\tilde{t})\right)\right\}$$
$$=\tilde{p}^{(1)}(n-\tfrac{1}{2},\tilde{\nu},\tilde{t})-\tilde{p}^{(1)}(n+\tfrac{1}{2},\tilde{\nu},\tilde{t})-\frac{1}{2}\left(\frac{\partial\tilde{p}^{(0)}}{\partial\tilde{\nu}}(n+\tfrac{1}{2},\tilde{\nu},\tilde{t})+\frac{\partial\tilde{p}^{(0)}}{\partial\tilde{\nu}}(n-\tfrac{1}{2},\tilde{\nu},\tilde{t})\right). \quad \text{(B.15)}$$

The solvability condition (the average of (B.15) over a period) becomes

$$\overline{\mu_{n+1/2}l^{(0)}(n+\tfrac{1}{2},\tilde{\nu},\tilde{t})}\tilde{u}^{(0)}(\tilde{\nu},\tilde{t})-\tilde{V}\overline{\left(\delta_{n+1/2}\frac{\partial^2 l^{(0)}}{\partial\tilde{t}\partial\tilde{\nu}}(n+\tfrac{1}{2},\tilde{\nu},\tilde{t})\right)}=-\frac{\partial\overline{\tilde{p}^{(0)}}}{\partial\tilde{\nu}}(\tilde{\nu},\tilde{t}),$$

which using (B.13) gives

$$\overline{\mu_{n+1/2}l^{(0)}(n+\tfrac{1}{2},\tilde{\nu},\tilde{t})}\tilde{u}^{(0)}(\tilde{\nu},\tilde{t})=-\frac{\partial A^{(0)}}{\partial\tilde{\nu}}(\tilde{\nu},\tilde{t}). \quad \text{(B.16)}$$

To leading order, the (2.18) for the end vertices become

$$\tilde{p}^{(0)}(\tfrac{1}{2},0,\tilde{t})-\tilde{V}\delta_{1/2}\frac{\partial l^{(0)}}{\partial\tilde{t}}(\tfrac{1}{2},0,\tilde{t})=0,\qquad \tilde{p}^{(0)}(N-\tfrac{1}{2},1,\tilde{t})-\tilde{V}\delta_{N-1/2}\frac{\partial l^{(0)}}{\partial\tilde{t}}(N-\tfrac{1}{2},1,\tilde{t})=0,$$

and so the boundary conditions for this approximation are

$$A^{(0)}(0,\tilde{t})=A^{(0)}(1,\tilde{t})=0. \quad \text{(B.17)}$$

In summary, assuming that the $\mu_{n+1/2}$ are not correlated with the other cellular parameters, by eliminating $A^{(0)}$ from (B.7), (B.8), (B.14) and (B.16), we obtain the system of equations (3.5a)–(3.5c) (with $\tilde{u}$ replaced by $\tilde{u}^{(0)}$, $\bar{l}$ replaced by $\overline{l^{(0)}}$, $\tilde{p}$ replaced by $\tilde{p}^{(0)}$, etc.). To close this system of equations we need a relationship between the mean cell lengths and the weighted average pressure appearing in (B.14); from (B.7), (B.12) and (B.14) we obtain the system of equations (3.5d), and the appropriate average pressure is given by (3.5e). The boundary conditions (3.6) are given from (B.7), (B.14) and (B.17).